Heat Wave Variability in the Southeast United States

Undergraduate Honors Thesis

Mitchell Voelker,

Meteorology Program

Department of Earth, Ocean, and Atmospheric Science,

Florida State University

Spring 2025

Honors Thesis Committee members:

Dr. Vasubandhu Misra

Dept. of Earth, Ocean, and Atmospheric Science

Dr. Jeffrey Chagnon

Dept. of Earth, Ocean, and Atmospheric Science

Dr. Bhargav Karamched

Dept. of Mathematics

TABLE OF CONTENTS

1. ABSTRACT

This study was motivated to assess the variability of the heat wave season in the Southeast United States from a 103 year (1903-2005) long downscaled atmospheric reanalysis of 10 km grid resolution. A heat wave day was defined as a day in which the maximum hourly heat index measurement for a particular location reached a value of 90°F or more. The heat waves were classified based on their duration as 1-day, 2-day, 3-day, 4-day, and a 5-day event.

The heat wave season is characterized by a few parameters in this study: the total number of heat wave events per year (season events), the first day a heat wave occurs in a year (season onset), the last day a heat wave occurs in a year (season demise), and the season length in a year (season demise minus season onset gives season length). The heat wave season interannual variability was determined by examining changes in the frequency of the heat wave events in the seasonal onset, seasonal demise, and seasonal length. The variations of the heat wave season are compared separately with June-July-August (JJA) seasonal anomalies of El Nino Index, the Bermuda High Index in the JJA season, and the gradient of anomalous sea surface temperatures (SSTs) between the Atlantic and East Pacific Ocean (Atlantic SST minus East Pacific SST) in the March-April-May (MAM) and JJA seasons.

The results suggest that the 1-day to 3-day heat waves are widely prevalent across southeastern US with 4-day and 5-day heat wave events limited to eastern Texas, Louisiana, southern Mississippi, southern Alabama, and southern Georgia. The earliest season onset occurs in the southern latitudes of south Florida and southeastern Texas, the next earliest occurs along the Gulf Coast, and finally North of the Gulf Coast. Similarly to the season onset, the latest season demise occurs in the southern latitudes of south Florida and southeastern Texas, the next latest occurs along the Gulf Coast, and finally North of the Gulf Coast. Since season onset and

season demise follow the same distribution pattern, the season length also follows this pattern. In all the heat wave parameters there is a climatology that establishes a gradient in which higher values are in the West and lower values are in the East.

Heat waves in the southeastern US display significant interannual variability. In other words, the heat wave parameters deviate from the expected climatology from year to year. The large-scale drivers of ENSO variations, Bermuda high variations, and the SST gradient between the tropical Atlantic and Pacific oceans show a varied and spatially discontinuous influence on heat waves. This suggests that in the absence of strong large-scale drivers, the heat wave seasonal variability is dictated largely by internal variations.

2. INTRODUCTION

Heat waves are an important weather phenomenon to investigate due to their danger to human health. In the United States, NOAA recognizes heat as the leading cause of weather-related deaths with 207 occurrences in 2023 (US Department of Commerce, NOAA). The European heat wave event of 2003 is one example of how heat waves can be extremely dangerous and even deadly. The European heat wave disaster led to a death toll between 22,000 and 35,000 people in 18 countries, with nearly 15,000 deaths in France alone as well as an estimated $13 billion (U.S. dollars) in costs (Fennessy and Kinter 2011). In general, heat waves place a heavier burden on people who have pre-existing medical conditions, are socially isolated, or do not have air conditioning (Semenza et al. 1996). In Europe, it is very common for residents to not have air conditioning because the region generally does not experience intense heat waves. However, in the case–control study conducted by Semenza et al. (1996) it was estimated that "more than 50 percent of the deaths related to heat waves could have been prevented if air conditioning had been present." The Southeast United States (SEUS), on the other hand, experiences many heat waves, but most residents in the SEUS have access to air conditioning. Poor, low-income individuals that do not have access to air conditioning and the elderly demography that tend to have medical conditions are vulnerable to heat waves. Furthermore, both groups are more socially isolated, which is another indicator of vulnerability to heat waves. The risk is also elevated for people who work for extensive periods of time outside like construction workers because although they may have air conditioning at home, they do not have it when they must work outside in extreme heat. "The heat stress placed on construction workers can have progressive effects on workers' health ranging from heat rash, heat cramp, heat fainting, heat exhaustion to heatstroke, leading to morbidity and mortality" (Rameezdeen and

Elmualim 2017). Seasonal predictability of the heat wave season will help construction companies prepare for summer seasons that are exceptionally hot, so that the companies can protect workers from heat stress while maximizing productivity at the construction site.

This study aims to determine the variability of heat waves in the SEUS. Gaining an understanding of the variability in a heat wave season allows meteorologists to determine how heat wave characteristics, such as the season onset or the heat wave frequency, are changing in a changing global climate. In some locations, the heat wave characteristics could be changing considerably and at other locations the characteristics could be constant, but the way to determine the extent of change is to determine if the change is outside of the expected variability due to internal variability or large-scale forcing of interannual variability. Some studies claim that there have been changes in the heat wave season at certain locations that are not driven by natural variability. For instance, in China there has been a significant increase in the number of heat wave events and annual heat wave days since the year 2000 (Li et al. 2021). Li et al. (2021) suggests the increase in heat wave days and events is a result of warming from greenhouse gases, changes in atmospheric circulation anomalies, and urbanization effects.

In the SEUS, it is important to consider how the rainy season and heat wave season intersect. “The SEUS is humid and subtropical, ensuring constant delivery of summer rainfall” (Selman and Misra 2016). However, the climate is generally more humid in the East and drier in the West due to two different air masses that affect the SEUS. The marine tropical (mT) air mass is a warm and humid air mass that originates in the Caribbean Sea, so it has the largest influence along the coast of the Gulf of Mexico and the eastern part of the SEUS. On the other hand, the continental tropical (cT) air mass is a hot and dry air mass that originates in Mexico and the Southwest United States. Therefore, Texas and Oklahoma have a drier climate in the boreal

summer season than the Deep South and Florida ("Air Masses and Fronts" n.d.). However, air masses shift due to internal variability of the weather system and due to the large-scale drivers of climate variability like ENSO. If dry air takes hold of the SEUS in boreal summer, temperatures are driven higher as subsidence builds over the region and this hot, dry air can stay in place for an extended period leading to a long duration heat wave. For example, a series of 1952 heat waves in the SEUS were characterized by a deeper-than-normal trough along the West Coast and a stronger-than-normal ridge in the Mississippi Valley. These atmospheric conditions were ideal for generating and maintaining transport of an unusually large volume of warm air from the southwest desert region to the central U.S., which drove the heat wave (Klein 1952). In general, this blocking pattern that sets up due to strong, relatively stationary ridges are the main features that drive long duration heat waves from North Florida to Texas.

Florida is a unique state in the SEUS due to its two distinct climates in North Florida and South Florida. Heat waves in northern Florida are primarily driven by large-scale continental ridging, while heat waves in central and southern Florida are caused by a combination of a continental ridge and a westward extension of the Bermuda–Azores high (Cloutier-Bisbee et al. 2019). Apart from South Florida, heat waves in the SEUS are driven entirely by general blocking patterns. Thus, the seasonal predictability of the heat wave season means being able to predict a numbered range of the long-lasting ridges that will set up in the SEUS. Trying to determine how large-scale drivers of climate variability alter these ridging patterns is the goal of heat wave variability research in the SEUS. Furthermore, "the instantaneous state of the weather system is reliable up to about 10 days" (ECMWF 2018). Thus, long-term predictions are made on a time scale of two or more weeks out, and long-term forecasters point to the likelihoods that are expected in sub-seasonal to seasonal forecasts. Even though climate variability forecasts rely on

explaining the expected long-term weather patterns and do not have the detailed weather story that is provided in an operational forecast, there is a strong societal desire to have forecast ability with a lead time of more than 10 days in advance. This desire is demonstrated by operational prediction centers like the climate prediction center (CPC) providing forecasts of seasonal mean climate for variables such as temperature and precipitation. These forecasts typically manifest as the expected departures from the seasonal climate mean, such as temperature anomalies expected in 2 weeks or how many more heat waves than normal are expected in the season. The hope of achieving sub-seasonal to seasonal predictability rests upon analyzing the variability driven by low-frequency variations, persistence of atmospheric regimes, and similar phenomena (Lorenz 1984). Even more optimism for determining the long-term variability of climate lies at analyzing the variability driven by slowly varying components such as sea surface temperature (SST), soil moisture, and albedo (Charney and Shukla 1981). The atmospheric regimes that are set up in response to the slowly varying components of SST that are investigated in this study are the ENSO index in JJA, the anomalous SST gradient between the Atlantic and Pacific in MAM, and the anomalous SST gradient between the Atlantic and Pacific in JJA. In addition, the influence of the variations of the Bermuda High Index (in JJA) on the heat waves is also investigated.

Increasing the understanding of climate variability and striving for seasonal predictability of the heat wave season offers potential benefits for resource planners. Despite potential benefits for resource planning, “there are obstacles to the extensive use of seasonal climate forecasts that include a lack of awareness of their existence, distrust of their accuracy, perceived irrelevance to management decisions, and competition from other technological innovations” (Carbone and Dow 2005). These obstacles have slowed the widespread deployment of utilizing climate variability to protect resources such as water. However, in the face of rapid industrial, residential,

and recreational growth in the SEUS, which has the fastest growing population in the country, demand for the resource of water has increased tremendously (Carbone and Dow 2005; Bastola et al. 2013). As water demand continues to grow and water systems confront quality issues, climate variability will play an increasingly important role in water resources management (Carbone and Dow 2005). Resource managers are now forced to employ seasonal predictions of climate variability. Another resource that the predictability of climate variability can protect is food security. In the SEUS farming is an integral part of the economy; In fact, agriculture is a multibillion-dollar industry in the SEUS and agricultural practices in the region do not rely heavily on irrigation, instead it is largely rain fed agriculture Bastola et al. 2013). Therefore, since heat waves are associated with extended periods of hot and dry weather, seasonal predictability of the heat wave season helps individuals whose livelihood depends on agriculture. For example, if seasonal predictability improves, farmers can increase productivity by better managing water resources.

3. METHODOLOGY

This study was motivated to assess the variability of the heat wave season in the Southeast United States from a 103 year (1903-2005) long downscaled atmospheric reanalysis of 10 km grid resolution. A heat wave day was defined as a day in which the maximum hourly heat index measurement for a particular location reached a value of 90°F or more. The heat waves were classified based on their duration as 1-day, 2-day, 3-day, 4-day, and a 5-day event. The heat wave season is characterized by a few parameters in this study: the total number of heat wave events per year (season events), the first day a heat wave occurs in a year (season onset), the last day a heat wave occurs in a year (season demise), and the season length in a year (season demise minus season onset gives season length). The data analyzed in this study establishes the climatology of these parameters, the variability of the parameters (not depending on large-scale drivers of climate variability), and the variability forced by large-scale drivers of climate variability.

There are various ways to define heat waves. There is consensus that a heat wave refers to an acute period of extreme warmth. Perkins et al. (2012) mentions that heat waves are loosely defined as a period, either consecutive days or single daily events, where conditions at or above the designated threshold of perceived warmth are achieved. Whereas the National Oceanic Atmospheric Administration (NOAA) defines a heat wave as a period of unusually hot weather lasting two or more days that exceeds the historical averages for the given area in that time of year (“NOAA SciJinks”).

In this study, heat wave was defined by setting a threshold to the heat index that must be met for a specified amount of time. The heat index was determined by equation (1).

$$I_{NWS} = -42.379 + 2.04901523T + 10.14333127R - 0.22475541TR - 0.00683783T2 - 0.05481717R2 + 0.00122874T2R + 0.0\,0085282T2R2 - 0.00000199T2R2 - - - - - (1)$$

Where I_{NWS}, T, and R represent heat index in °F, the temperature in °F, and relative humidity in percentage. I_{NWS} is calculated each hour throughout the day and the daily maximum I_{NWS} is classified into one of four categories HI13 through HI16 (Table 1).

An adjustment to I_{NWS} (I^{*}_{NWS}) computed from Equation 1 is made when R is less than 13% and T is between 80°F and 112°F as:

$$\mathrm{I^{*}_{NWS}} = \mathrm{I_{NWS}} - \mathrm{B} - - - - - - - - - - - - - - - (2)$$

$$B = \frac{(13 - \mathrm{R})}{4}\sqrt{\frac{17 - |T - 95|}{17}} - - - - - - - - - - - - - - - - (3)$$

However, if R is greater than 85% and T is greater than 80°F but less than 87°F then B takes the form:

$$B = \left(\frac{R - 85}{10}\right) \cdot \left(\frac{87 - T}{5}\right) - - - - - - - - - - - - - - - (4)$$

Since I_{NWS} is calculated each hour throughout the day, this study used the daily maximum I_{NWS} obtained in a day to determine the occurrence of a heat wave at an arbitrary location. As seen in Table 1, the category of HI14 is achieved if the maximum heat index measurement reaches 90°F. In this study, HI14 heat waves of 1-day, 2-day, 3-day, 4-day, and 5-day durations were analyzed. For the 1-day heat wave duration, any time the maximum heat index measurement reached 90°F or above, it was considered a heat wave. For the 2-day heat

wave duration 2 consecutive days had to have a maximum heat index measurement that reached 90°F or above. For the 3-day heat wave duration 3 consecutive days had to have a maximum heat index measurement that reached 90°F or above. The same logic was used for the 4-day and 5-day heat wave durations. It is important to note that the heat waves were not grouped independently; A 3-day heat wave means that there are three 1-day heat waves and there is one 2-day heat wave. Another example is that a 5-day heat wave means that there are five 1-day heat waves, there are two 2-day heat waves, there is one 3-day heat wave, and there is one 4-day heat wave. If there happened to be no heat waves in a year for a given heat wave duration at a given grid point (pixelated location) then I designated that grid point as NaN (not a number). Therefore, in the 100-year 5-panel plots if any year at a particular grid point out of the 100 years does not have data, there is no data for that grid point in the 100-year 5-panel plot. That is the reason that some data available at the 1-day heat wave subplot is not available progressing toward long duration heat waves, such as the 5-day heat wave subplot.

Table 1 – Definitions of heat wave indices. Reproduced from Smith et al. (2013)

Heatwave index	**Temperature metric**	**Threshold**	**Duration**	**Type**	**Reference**
HI01	Mean daily temperature	95th percentile	2+ consecutive days	Relative	Anderson and Bell (2011)
HI02	Mean daily temperature	90th percentile	2+ consecutive days	Relative	Anderson and Bell (2011)
HI03	Mean daily temperature	98th percentile	2+ consecutive days	Relative	Anderson and Bell (2011)
HI04	Mean daily temperature	99th percentile	2+ consecutive days	Relative	Anderson and Bell (2011)
HI05	Minimum daily temperature	95th percentile	2+ consecutive days	Relative	Anderson and Bell (2011)

HI06	Maximum daily temperature	95th percentile	2+ consecutive days	Relative	Anderson and Bell (2011)
HI07	Maximum daily temperature	T1 > 81st percentile T2 > 97.5th percentile	1. Everyday > T1 2. 3+ consecutive days > T2 3. Avg Tmax > T1 for the whole time period	Relative	Peng et al. (2011); Meehl and Tebaldi (2004)
HI11	Maximum daily temperature	35°C		Absolute	Tan et al. (2007)
HI12	Minimum and maximum daily temperature	Tmin ≥26.7°C Tmax ≥40.6°C	At least one of the thresholds to be met for 2+ consecutive days	Absolute	Robinson (2001)
$HI13^{+}$	Maximum daily heat index	80°F	1 day	Absolute	NWS; Rothfusz and Scientific Services Division (1990); Steadman (1979)
$HI14^{+}$	Maximum daily heat index	90°F	1 day	Absolute	NWS; Rothfusz and Scientific Services Division (1990); Steadman (1979)
$HI15^{+}$	Maximum daily heat index	105°F	1 day	Absolute	NWS; Rothfusz and Scientific Services Division (1990); Steadman (1979)

$HI16^{+}$	Maximum daily heat index	130°F	1 day	Absolute	NWS; Rothfusz and Scientific Services Division (1990); Steadman (1979)

+ Uses the I_{NWS} index provided in Equation 1 in the text.

Note that the HI08, HI09, and HI10 are not included because that heat index uses apparent temperature as the threshold, and apparent temperature was not used in this study so there is no need to define it.

4. RESULTS

i. General heat Wave Characteristics in the Southeast United States

Figure 1 shows the climatological average number of heat wave events that occur in a heat wave season. Figure 1a indicates that the highest number of 1-day heat waves occur in southeastern Texas, northern Louisiana, southern Alabama, southern Mississippi, southern Georgia, and Florida. In Florida the highest number of heat waves occur away from the coast, with increasing frequency towards North Florida (Figure 1a). The 1 to 5-day duration heat wave events display a zonal gradient with higher frequency in the west relative to the east in the southeastern United States (Figure 1). Furthermore, southern Texas has the highest number of heat wave events, regardless of the duration of the heat wave. Whereas Florida displays the least frequency of the 4 and 5-day heat wave events relative to other neighboring states in the southeastern United States (Figure 1).

The climatological date of the first 1-day heat wave of the season is shown in Figure 2a, which shows that the heat wave season begins earliest in the southern part of the southeastern United States. Figure 2a shows that southern Texas has the earliest start to the 1-day heat wave season, while Central Florida, southern regions of Louisiana, Alabama, Mississippi, and Georgia have a notably early start to the 1-day heat wave season. Figure 2b, which shows the onset of the 2-day heat wave season, has similar patterns to the 1-day heat wave season. However, in the long duration (3-day, 4-day, and 5-day) heat waves, shown by Figure 3c, 3d, and 3e, the earliest start to the heat wave season becomes confined to southern Texas.

The climatological date of the last 1-day heat wave of the season is shown in Figure 3a, which shows that the heat wave season ends the earliest in the northern parts of the domain and

latest in southern parts of the domain. Southern Texas has the latest end to the 1-day heat wave season, while regions along the Gulf Coast as well as Florida have a notably late demise to the 1-day heat wave season (Figure 3a). The demise of the 2-day heat wave season, shown by Figure 3b, has similar trends to the demise of the 1-day heat wave season with regions like Central and West Florida, the far western part of the Florida Panhandle, Coastal Alabama and Mississippi, Central Louisiana, and southern Texas having a notably late demise to the 2-day heat wave season. In the long duration (3-day, 4-day, and 5-day) heat waves, shown by Figure 3c, 3d, 3e, the latest end to the heat wave season is confined to Texas.

Figure 4, which shows the length of the heat wave season marked by their different durations indicate that the heat wave season is very long in southern parts relative to the northern regions of the southeastern United States. Since the first 1-day heat wave occurs very early and the last 1-day heat wave occurs very late in the year, the 1-day heat wave season is longest relative to other long duration heat wave events (Figure 4). Figure 4a shows that Southern Texas has the longest 1-day heat wave season, and other regions with notably long 1-day heat wave seasons include the Gulf Coast of the United States and Florida. A similar trend is observed in Figure 4b. However, long duration heat waves are less frequent in Florida because of the high prevalence of rain in the summer (wet) season that break up the days in a row of heat which are required for the 3-day, 4-day, and 5-day heat waves. In the long duration heat waves, shown by Figure 4c, 4d, and 4e, Southern Texas has an exceptionally long heat wave season, the Deep South, and the Gulf Coast (outside of Florida) has a notably long heat wave season.

ii. Interannual Variability of Heat Waves in the Southeast United States

Figures 5-8 show that there is significant variability in the heat wave season from year to year. Some of this variability is driven by large-scale drivers of ENSO variations, Bermuda High

variations, and the SST gradient between the tropical Atlantic and Pacific. However, the variability could also be driven by internal chaotic variations of the weather and climate system. For instance, figure 5a shows that in a small region of the United States – northeastern Texas and southeastern Oklahoma – the standard deviation is within the range of 36 – 54 for one day heat wave events per year. Another region that has large interannual variations is Central and Northern Florida with a peak along the Big Bend region of Florida. The patterns highlighted for one-day heat waves continue for long duration heat waves, but the variations diminish in each successive heat wave duration (Figures 5b-e). This is due to the available data gradually becoming confined to southern parts of the domain and the data that is available is generally of smaller magnitude because there are fewer total heat waves of long duration than short duration.

In Figure 6, Florida and Texas show a large standard deviation of the heat wave season onset (in days) over the 100 years (1904 – 2004), while the rest of the domain show comparatively far less variations. This suggests that the onset of the heat wave season is strongly tied to the seasonal cycle outside of Texas and Florida. Similarly, in Figure 7, Florida and Texas have larger standard deviations of the heat wave season demise (in days) over 100 years (1904 – 2004) compared to the rest of the southeastern United States. Although in comparison to Figure 6, the variations of the demise date of the heat wave season are much smaller, which suggests that the demise is more strongly anchored to the seasonal cycle than the onset of the heat wave season. Consequently, Florida and Texas display relatively larger standard deviations of the heat wave season length (in days) over 100 years (1904 – 2004) than the rest of the southeastern United States (Figure 8).

iii. Large-scale Drivers of Interannual Heat Wave Variability in the Southeast United States

The large-scale drivers of interannual heat wave variability in the southeastern United States are important teleconnections to investigate as they offer hope for seasonal predictability. In this study we examine the influence of the following large-scale drivers of interannual heat wave variability: variations of ENSO, variations of the Bermuda High Index, and the variations in the SST gradient between the tropical Atlantic and Pacific for March, April, and May (MAM), as well as June, July, and August (JJA) seasons.

The ENSO variations are captured by the seasonally averaged SST in the Nino 3.4 region (5N-5S and 150W-90W). In Figure 9, we show the regression of the frequency of heat wave events per year on the mean Nino3.4 SST index in the JJA season, with the stippling indicating that it is statistically significant at the 90% confidence interval. We find in Figure 9a that the ENSO teleconnections on the heat wave frequency in the southeastern United States are weak (only northeastern Louisiana displays a statistically significant negative regression for the 1-day heat wave event) in the boreal summer season. The other heat wave duration regressions do not have a significant bearing on the frequency of heat waves observed in a season. It is well known that ENSO teleconnections in the southeastern United States are weak in the summer season when the subtropical jet in the upper troposphere has moved further poleward (Lee et al. 2009). Similarly, in the short duration ($\leq$ 2 day) heat wave season we find that the regression of the heat wave season onset with ENSO variations in the JJA season is very weak. Although, in the 2-day heat wave duration (Figure 10b) there are weak statistically significant positive regressions in a small region of Central Florida and Central Texas. However, in the long duration ($\geq$ 3 day) heat wave season ENSO variations in the JJA season have significant bearing on the onset of the heat wave season. For instance, Figure 10d shows a statistically significant negative regression in eastern Texas and northeastern Louisiana. Similarly to the season onset regression, the season

demise regression shows positive values in the short duration (≤ 2 day) heat waves. Figure 11a shows statistically significant positive regressions in Texas, northern Louisiana, Arkansas, and eastern Oklahoma. In Figure 11b the positive regressions become comparatively much weaker. In the long duration (≥ 3 day) heat waves, the regression values become negative. Figure 11c shows a statistically significant negative regression in the western Florida Panhandle and southern Texas. Figures 11d and 11e both show a statistically significant negative regression in northern Louisiana, southern Arkansas, and southern Alabama. The heat wave season length regression with the Nino3.4 index in the JJA season continues the pattern of short duration (≤ 2 day) heat waves having more positive regression values that switch to negative regression values in the long duration (≥ 3 day) heat waves. According to Figure 12, The ENSO variations in JJA have the strongest impact on the length of the heat wave season in eastern Texas. Figure 12b shows a statistically significant positive regression in eastern Texas, suggesting that a warm ENSO event in JJA is associated with a longer heat wave season. However, in the 3-day duration heat wave the regression value flips to negative in eastern Texas (Figure 12c) meaning that a warm ENSO event in JJA is associated with a shorter heat wave season.

The variations in the Bermuda High Index as measured by the sea-level pressure gradient between 90W and 78W along 30N has a more extensive influence on the frequency of heat wave events (Figure 13) than ENSO variations (Figure 9). For example, in Figure 13a the entire southeastern United States, except Texas, has a statistically significant negative regression meaning that a positive zonal gradient of the sea level pressure along 30N is associated with a lower frequency of the 1-day heat wave events. However, these regressions become less extensive for the long duration heat wave events (Figures 13b-e). In fact, over northern Mississippi, southern Louisiana, and northern Alabama for 3-day heat wave events (Figure 13c)

and over eastern Texas for the 4-day heat wave events (Figure 13d), the signs of these statistically significant regressions reverse relative to Figure 13a; Thus, these regions have positive regressions for their respective heat wave durations. In other words, in these regions if there is a positive zonal gradient along 30N there is an associated higher frequency of (3 and 4-day) heat wave events. Like the ENSO variations, the variability of the Bermuda High has less of an extensive influence on the onset (Figure 14) and demise (Figure 15) than the length (Figure 16) of the heat wave season. The 1-day heat wave season onset regression with the Bermuda High Index (Figure 14a) shows a statistically significant positive regression in South Florida and the 2-day heat wave regression (Figure 14b) shows a statistically significant positive regression in Central Texas. However, in the long duration heat wave regressions (Figures 14c – 14e) the sign of the regression flips relative to the short duration heat waves. For instance, Figure 14c shows the strongest statistically significant negative regression in Texas with Mississippi, Alabama, and Georgia observing comparatively weaker negative regressions. The 1-day heat wave season demise regression with the Bermuda High Index (Figure 15a) shows an extensive region of statistically significant negative regressions; These regressions are observed in northern Louisiana, the Texas side of the border with northern Louisiana, Florida, and southern Georgia. However, in the long duration heat wave events the regions of negative statistical significance become centered on the Gulf Coast of Texas which is illustrated by the 4-day heat wave duration plot (Figure 15d). Similarly to the variations of ENSO, the variability of the Bermuda High has an influence on the heat wave season length that affects large regions of the Southeast Unted States. In the 1-day heat wave season length regression with the Bermuda High Index (Figure 16a) there is a statistically significant negative regression in Texas that extends North into Central Oklahoma. However, in the long duration heat waves the sign of the regression flips. For

instance, in the 2-day heat wave duration (Figure 16b) there is a statistically significant positive regression in Texas, Northeast Louisiana, Arkansas, and East Oklahoma. The 4-day heat wave duration (Figure 16d) shows the positive regression in Texas, North Louisiana, South Mississippi, South Alabama, and Southeast Georgia.

The SST gradients between the Atlantic and the East Pacific Ocean are computed as the difference in area averaged SST between 10N-25N and 80W and 40W in the Atlantic and 0-10N and 160E -160W in the Pacific Ocean (Atlantic SST minus Pacific SST). These SST gradients are computed separately as the seasonal average for MAM and JJA seasons. Figures 17-20 show the regressions of the heat wave parameters (frequency, season onset, season demise, and season length) on the MAM averaged SST gradient between the two ocean basins while Figures 21-24 show the same regressions for the JJA averaged SST gradient. The influence of the variations of the SST gradients between the two ocean basins are comparatively weak relative to either the ENSO variations or the Bermuda High variations. However, there are some instances when this teleconnection becomes prominent. In the regression of 1-day heat wave frequency with the MAM averaged SSTs there is a statistically significant positive regression over the Carolinas (Figure 17a). In the onset regression there are weak negative regression values in shorter heat wave durations (≤ 3 days) but a transition to positive regression values occurs in the longer heat waves (≥ 4 days). For instance, in Figure 18d there are statistically significant positive regression values in southern Central Texas. In the demise regression, statistically significant values show up in the long duration heat wave events (≥ 4 days) with Figure 19d showing a negative value in southern Texas and Figure 19e showing a positive value in northern Louisiana, southeastern Mississippi, and southern Alabama. In the season length regression, statistically significant positive regression values are spatially incoherent in short duration heat waves (≤ 2 days), but in

long duration heat waves (≥ 3 days) positive values concentrate in Texas (Figure 20). The JJA SST gradient shows similar relationships with the heat wave season as the MAM SST gradient between the tropical Atlantic and Pacific. For instance, in the onset regression (Figure 22) weak negative regression values in shorter heat wave durations (≤ 3 days) transition to positive regression values in the long duration heat waves (≥ 4 days); This is illustrated in the 4-day heat wave duration which displays positive regression values in southern Central Texas (Figure 22d). Similarly, in the demise regression (Figure 23), the short duration heat waves (≤ 3 days) have weak regression values, but in the long duration heat waves (≥ 4 days) regression values strengthen. Figure 23e shows strong statistically significant positive regression values in northern Louisiana, southeastern Mississippi, and southern Alabama, which are the same regions that had positive values in the 5-day season demise regression for the MAM season (Figure 19e). Similarly to the season length for the MAM season, long duration heat waves (≥ 3 days) have statistically significant positive regression values that concentrate in Texas (Figure 24) with the 3-day heat wave having the strongest positive values in Texas (Figure 24c).

In the appendix section, the regression of the heat wave season parameters with the SST anomaly gradients between the Atlantic Ocean and the East Pacific Ocean are investigated. This was done to determine if these results differ from the regressions with SST gradients between the Atlantic and the East Pacific. The same seasons are investigated, so SST anomaly gradients are computed separately as the seasonal average for MAM and JJA seasons. The SST anomaly is defined as the MAM/JJA of a particular year minus MAM/JJA SST climatology. The SST anomaly gradient is computed as the difference in area averaged SST anomaly between 10N-25N and 80W and 40W in the Atlantic and 0-10N and 160E-160W in the Pacific Ocean (Atlantic SST anomaly minus Pacific SST anomaly). The figures (1.A to 8.A) in the appendix section

show that there is no significant difference between the regression of SST anomaly gradient with the heat wave season parameters and the regression of SST gradient with the heat wave season parameters. The same results are obtained when using either SST dataset.

5. CONCLUSIONS

This study was motivated to assess the variability of the heat wave season in the Southeast United States using a 103 year (1903-2005) long downscaled atmospheric reanalysis of 10 km grid resolution. This study uses this high-resolution atmospheric reanalysis dataset to analyze the heat wave seasonal climatology and its variability driven both by internal variations and by large scale drivers of climate variability that include ENSO, the Bermuda High Index, and the SST gradient between the tropical Atlantic and Pacific Oceans. Heat waves are an important severe weather event that results in significant mortality in the United States. In the Southeastern United States (SEUS), this weather phenomenon assumes more significance given that their season of occurrence is longer, the population of limited resource is significant, and there is considerable outdoor activity including farming and construction that exposes the workforce to its impacts.

This study finds that in the SEUS Texas has the highest number of heat waves regardless of heat wave duration. Florida has a considerable number of short (1-day to 3-day) duration heat waves. However, long (4-day and 5-day) duration heat waves are limited to Southeast Texas, Louisiana, southern Mississippi, southern Alabama, and southern Georgia. South Texas has the earliest heatwave events regardless of heat wave duration, while South Florida has a considerably early start to the short duration heat wave season. The next earliest onset of the heat wave season occurs along the Gulf Coast. Regions of the SEUS that have an early start to the heat wave season generally have a late end to the heat wave season. South Texas has the latest

season demise, while South Florida has a considerably late end to the short duration heat wave season. The next latest end to the heat wave season occurs along the Gulf Coast. Given these variations of the onset and demise of the heat wave season, it follows that the longest heat wave season occurs in South-Central and Southwestern Florida, the far Western Florida Panhandle, Coastal Alabama and Mississippi, Central Louisiana, and Southern Texas.

Quantifying the general variations of the heat wave season in the SEUS from this long period dataset is vital to understand the variability driven by large-scale drivers of climate variability. We find that the interannual variability of heat wave season characteristics decreases progressing from short to long duration heatwaves. However, some regions were an exception to this. For instance, Texas had high variability in the number of heat waves from year to year, regardless of whether long duration heat waves or short duration heat waves were analyzed. Furthermore, the onset and demise dates of the heat wave season as diagnosed by the occurrence of the first and the last heat wave episodes of the year have very small standard deviation except in Florida and Texas where it is relatively high. This suggests that in the southeastern US outside of Florida and Texas, the heat wave season is strongly tied to the seasonal cycle.

The large-scale drivers of ENSO variations, Bermuda high variations, and the SST gradient between the tropical Atlantic and Pacific oceans show a varied and spatially discontinuous influence on heat waves. The influence becomes especially noisy when comparing different heat wave durations to the effect of large-scale drivers of heat wave variability. In the Deep South (Louisiana, Mississippi, and Alabama), there is a statistically significant negative correlation between the ENSO index and the seasonal demise of the long (4-day and 5-day) duration heat waves. This means that if there is a positive anomaly (El Niño) in the Nino 3.4 region of the Pacific, then an earlier heat wave season demise is expected in the region.

Conversely, if there is a negative anomaly (La Niña), then a later heatwave season demise is expected.

The illusive influence of the large-scale drivers of climate on the heat waves in the SEUS is partly a result of its coincidence with the summer season, when the tropical oceans exhibit weaker SST gradients. Our analysis indicates from the lack of robust (or consistent and strong) correlations of the heat wave seasonal features with the large-scale climate indices that the heat wave variability in SEUS is potentially dictated by internal variations. This is understandable given that ENSO variability peaks in the boreal winter. Furthermore, the SST gradient between the tropical Atlantic and the Pacific is also strongest in boreal winter and spring seasons. Finally, the Bermuda High index is comparatively less variable than the other two large-scale SST based indices. Nonetheless, it has the most extensive correlations across the SEUS with 1-day heatwave events. But for higher duration heat wave events these correlations become less extensive and more local. These local relationships however are hard to explain.

6. ACKNOWLEDGEMENTS

Deep gratitude is extended to Dr. Vasubandhu Misra for his efforts in introducing me to research through the Undergraduate Research Opportunity Program (UROP) at Florida State. After I was introduced to Dr. Misra's research group through UROP, I began work on Directed Individual Studies (DIS) that served as the backbone for my results in this undergraduate thesis. I give sincere thanks for his guidance through my undergraduate honors thesis journey. I also express deep gratitude to postdoctoral researcher Dr. Jayasankar Balasubraman for his time and effort in helping me learn Python coding.

7. REFERENCES

"Air Masses and Fronts." *Air Masses and Fronts | METEO 3: Introductory Meteorology*, www.e-education.psu.edu/meteo3/l3_p5.html. Accessed 24 Jan. 2025.

Bastola, S., V. Misra, and H. Li, 2013: Seasonal Hydrological Forecasts for Watersheds over the Southeastern United States for the Boreal Summer and Fall Seasons. *Earth Interact.*, **17**, 1–22, https://doi.org/10.1175/2013EI000519.1.

Carbone, G. J., and K. Dow, 2005: Water resource management and drought forecasts in South Carolina. J Am Water Resour As. 41: 145–155

Charney, J. G., and J. Shukla, 1981: Predictability of monsoons. Monsoon Dynamics, J. Lighthill and R. P. Pearce, Eds., Cambridge University Press, 99–109.

Cloutier-Bisbee, S. R., A. Raghavendra, and S. M. Milrad, 2019: Heat Waves in Florida: Climatology, Trends, and Related Precipitation Events. J. Appl. Meteor. Climatol., **58**, 447–466, https://doi.org/10.1175/JAMC-D-18-0165.1.

Fennessy, M. J., and J. L. Kinter, III. "Climatic Feedbacks during the 2003 European Heat Wave". Journal of Climate 24.23 (2011): 5953-5967. < https://doi.org/10.1175/2011JCLI3523.1>. Web. 10 Jan. 2023

Klein, W. H. (1952), The weather and circulation of June 1952: A month with a record heat wave, *Mon. Weather Rev.*, **80**(6), 99–104.

Li, N., Z. Xiao, and L. Zhao, 2021: A Recent Increase in Long-Lived Heatwaves in China under the Joint Influence of South Asia and Western North Pacific Subtropical Highs. *J. Climate*, **34**, 7167–7179, https://doi.org/10.1175/JCLI-D-21-0014.1.

Lorenz, E.N., 1984: Some aspects of atmospheric predictability. Problems and Prospects in Long and Medium Range Weather Forecasting, D. M. Burridge and E. Kallen, Eds., Springer-Verlag, 1–20.

Rameezdeen, R., & Elmualim, A. (2017). The Impact of Heat Waves on Occurrence and Severity of Construction Accidents. *International Journal of Environmental Research and Public Health, 14*(1), 70. https://doi.org/10.3390/ijerph14010070

Semenza C. Jan, Ph.D., M.P.H., Rubin H. Carol, D.V.M., M.P.H., Falter H. Kenneth, Ph.D., Selanikio D. Joel, M.D., W. Dana Flanders, M.D., D.Sc., Howe L. Holly, Ph.D., and Wilhelm L. John, M.D., M.P.H., 1996. Heat-Related Deaths during the July 1995 Heat Wave in Chicago. The new England Journal of Medicine. https://www.nejm.org/doi/full/10.1056/NEJM199607113350203

US Department of Commerce, NOAA. “Weather Related Fatality and Injury Statistics.” National Weather Service, NOAA’s National Weather Service, www.weather.gov/hazstat/.

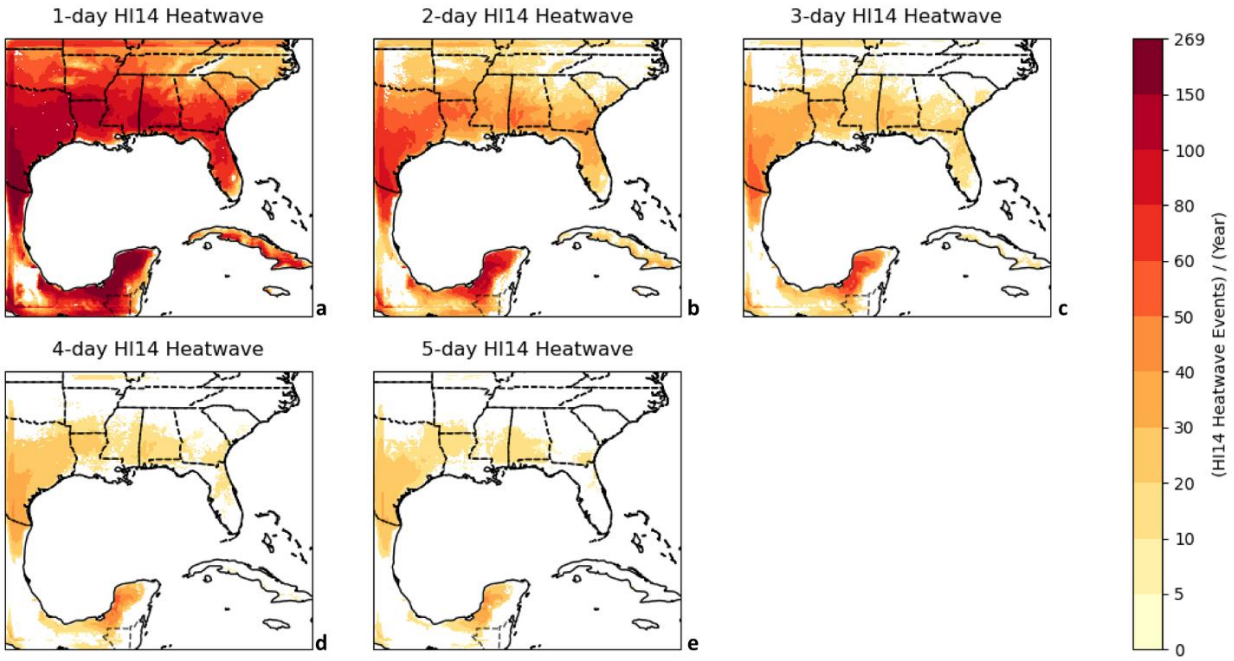

Figure 1: Climatological Average HI14 Heatwave Events per Year over 100 years (1904 – 2004)

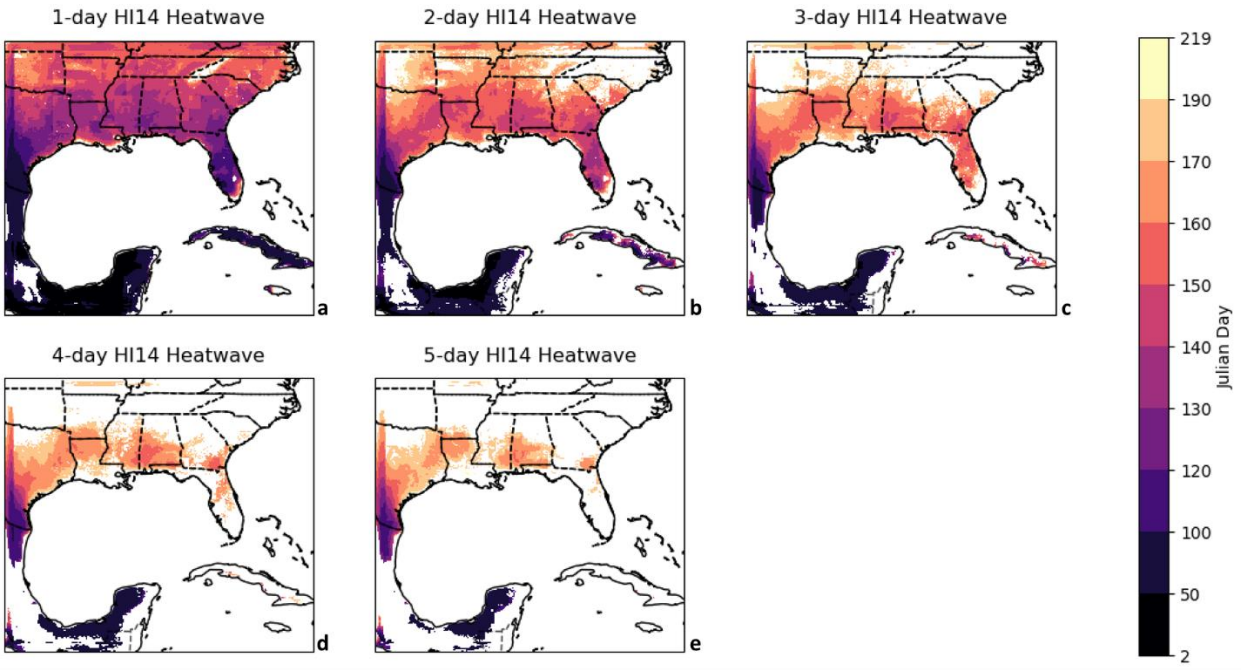

Figure 2: Climatological Average HI14 Heatwave Season Onset Date (in julian days) over 100 years (1904 – 2004)

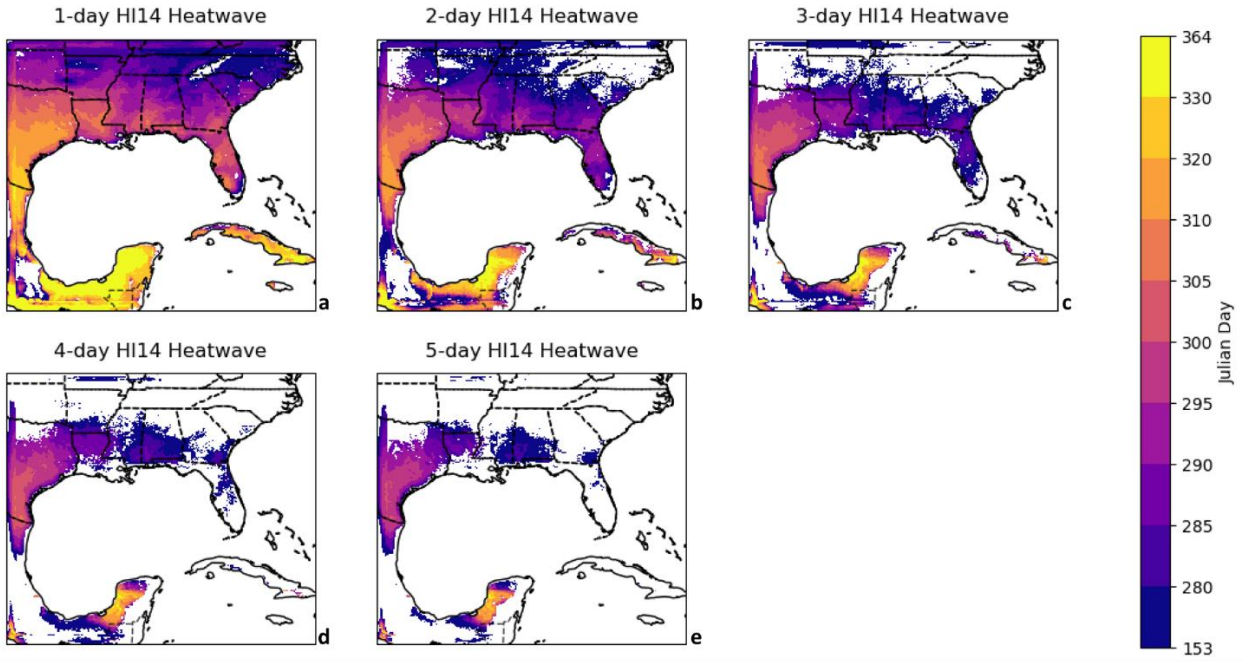

Figure 3: Climatological Average HI14 Heatwave Season Demise date (in julian days) over 100 years (1904 – 2004)

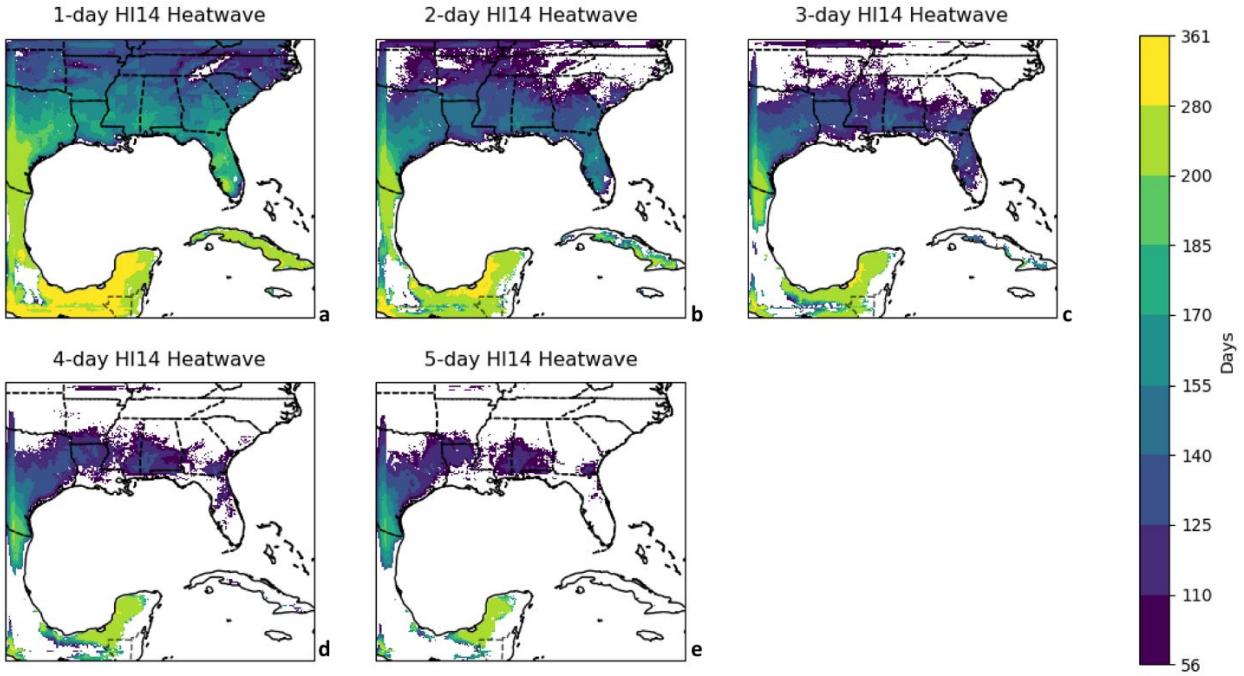

Figure 4: Climatological Average HI14 Heatwave Season Length (in days) over 100 years (1904 – 2004)

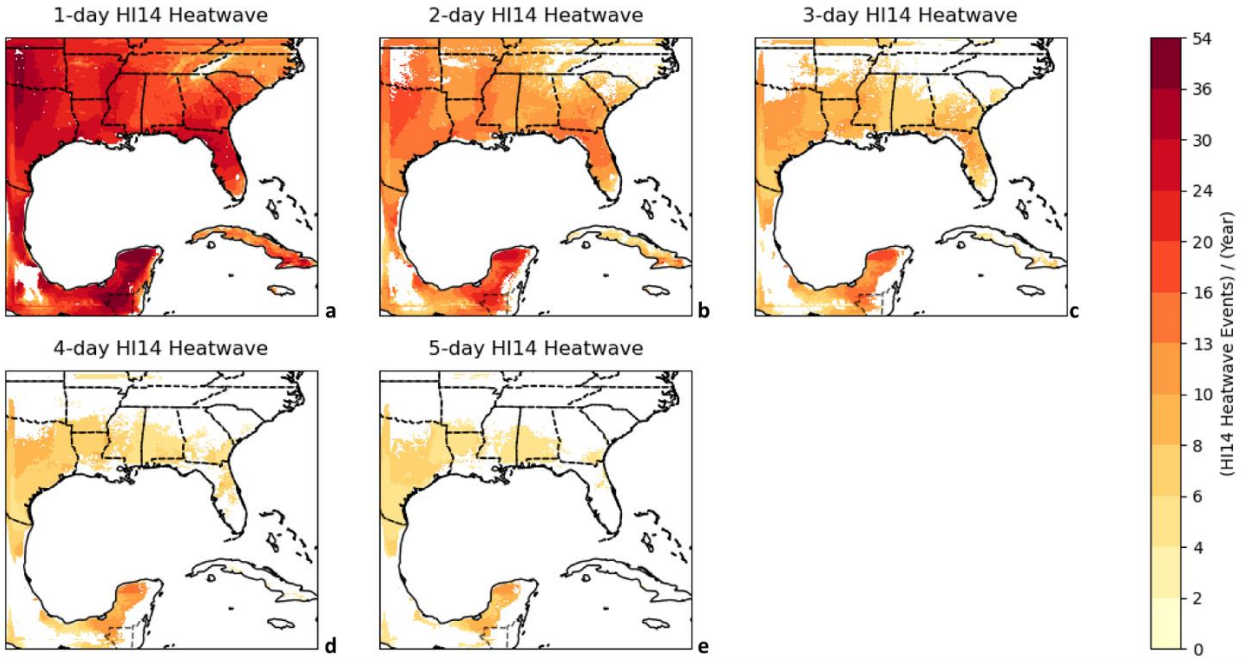

Figure 5: Standard Deviation of the HI14 Heatwave Events per Year over 100 years (1904 – 2004)

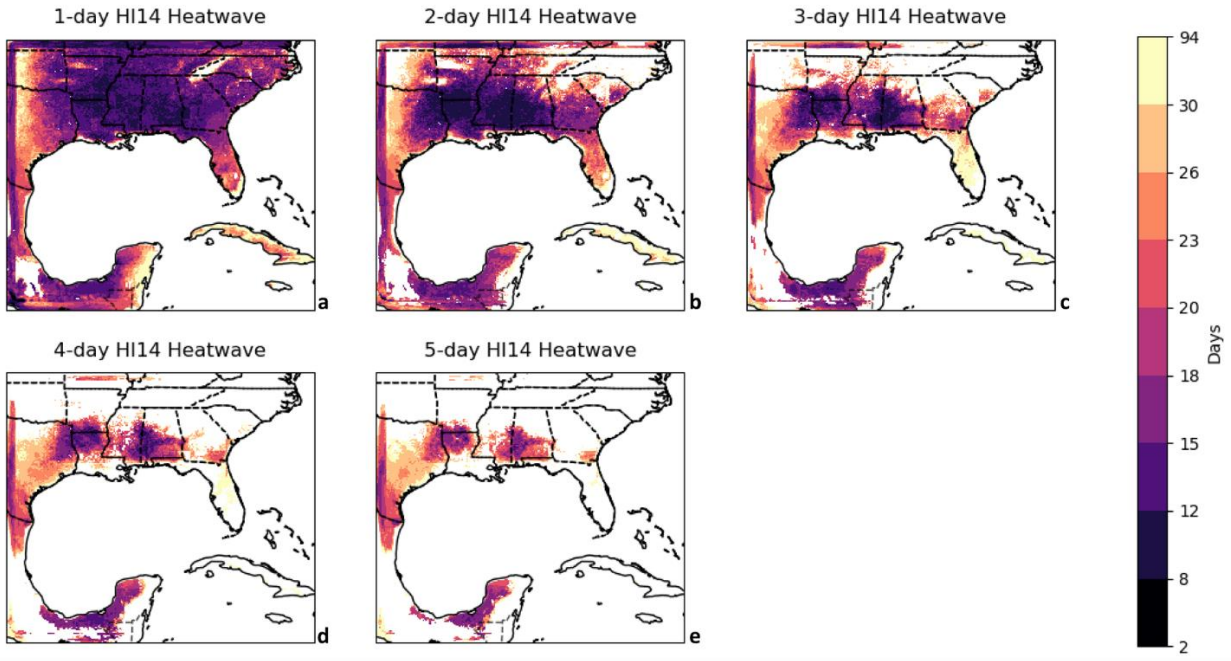

Figure 6: Standard Deviation of the HI14 Heatwave Season Onset (in days) over 100 years (1904 – 2004)

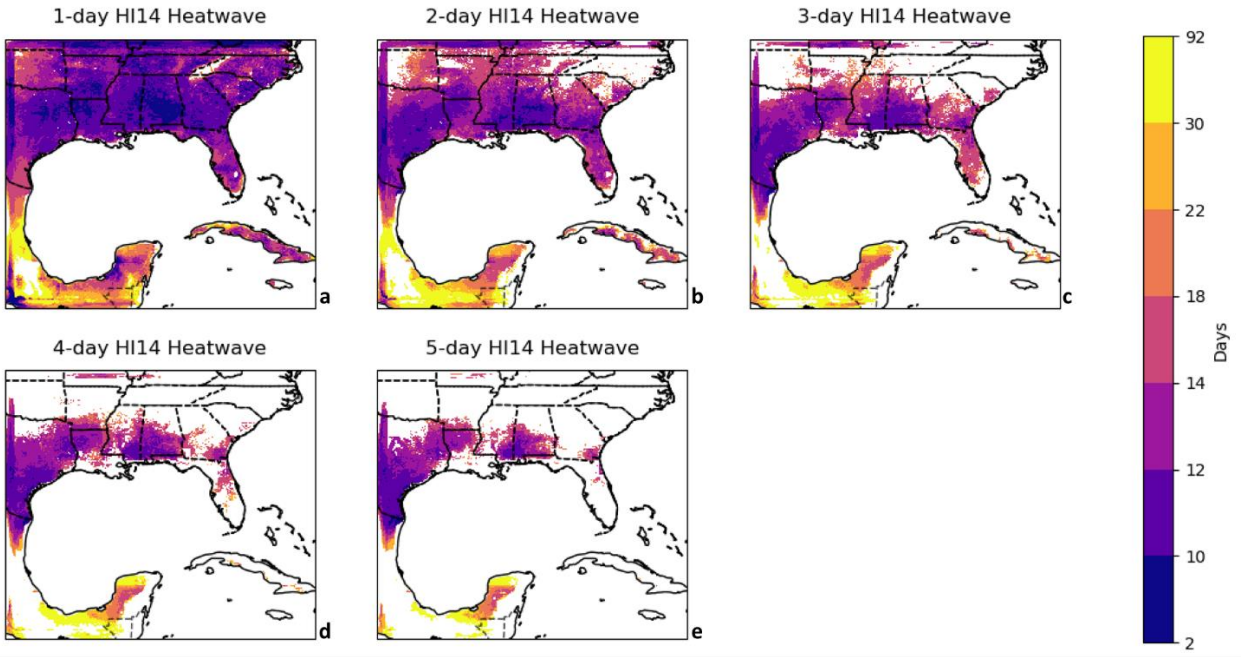

Figure 7: Standard deviation of the HI14 Heatwave Season Demise (in days) over 100 years (1904 – 2004)

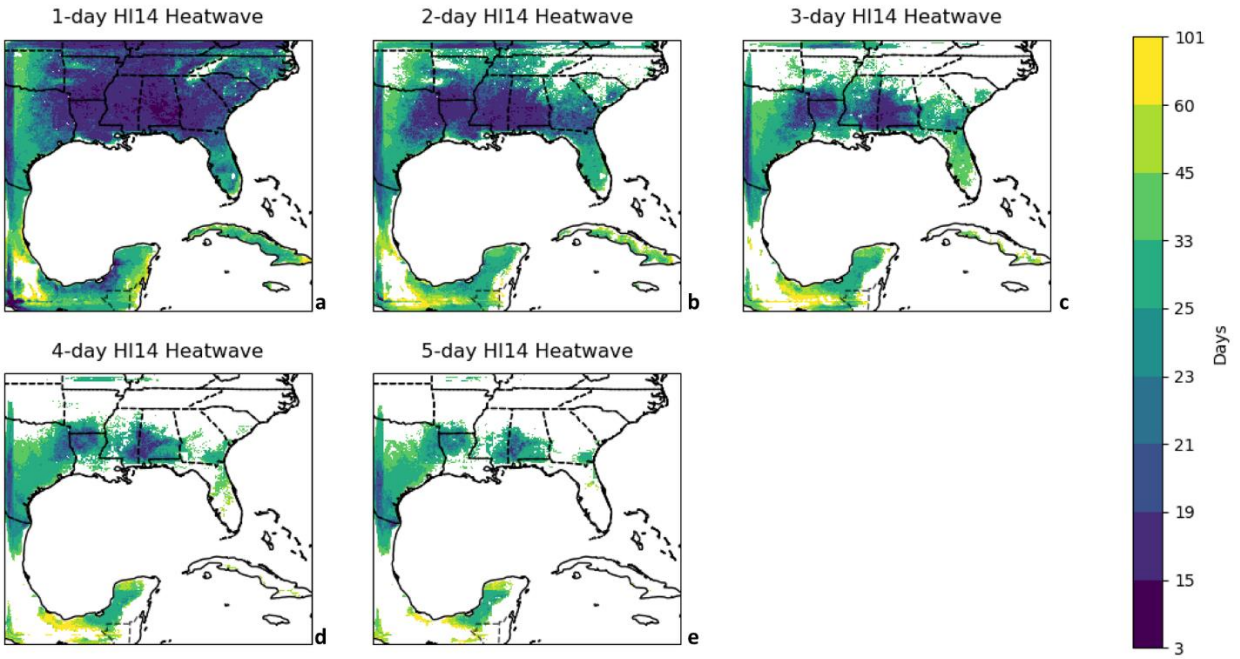

Figure 8: Standard Deviation of the HI14 Heatwave Season Length (in days) over 100 years (1904 – 2004)

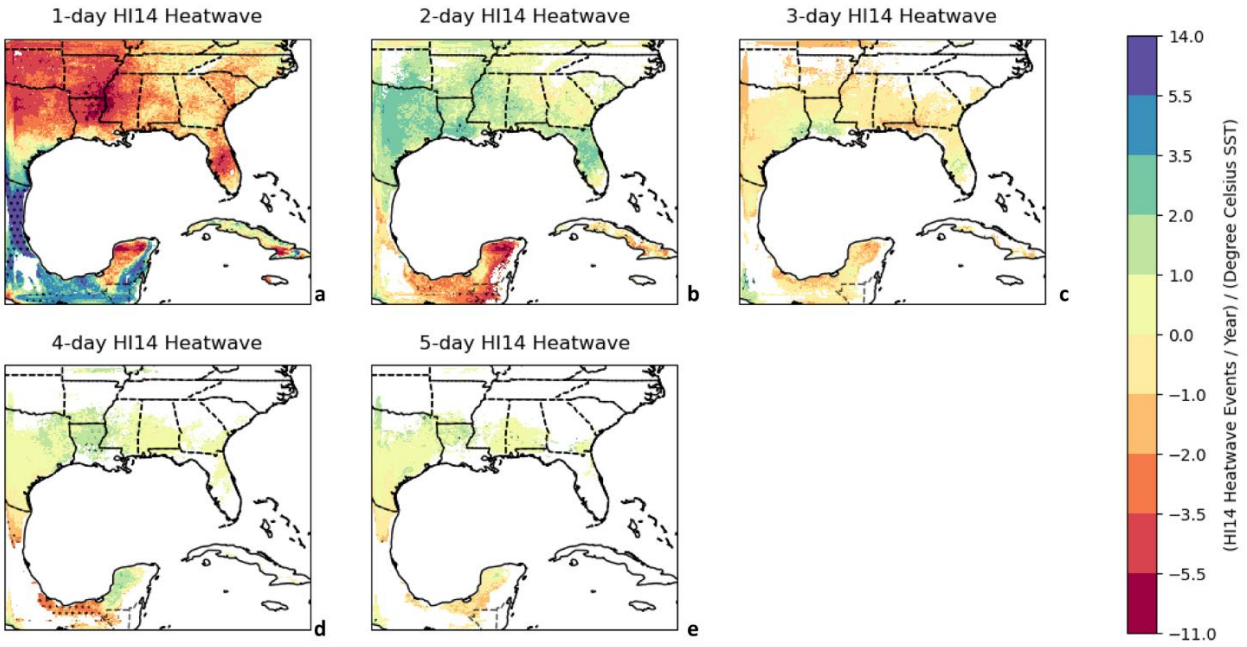

Figure 9: Linear Regression between HI14 Heatwave Events per Year and Average Degree Celsius Sea Surface Temperatures in the Nino 3.4 Region in June, July, August over 100 years (1904 – 2004). Black stippling patterns indicate that the slope value is statistically significant in the 90% confidence interval according to the two-tailed t-test.

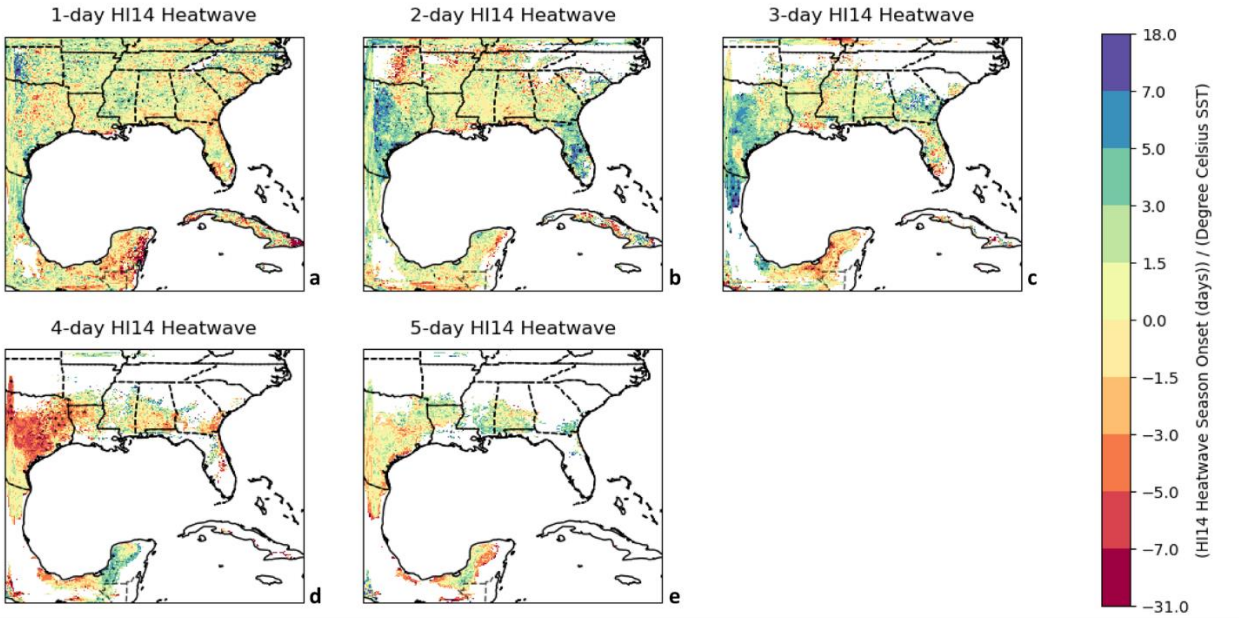

Figure 10: Linear Regression between HI14 Heatwave Season Onset (in days) and Average Degree Celsius Sea Surface Temperatures in the Nino 3.4 Region in June, July, and August over 100 years (1904 – 2004). Black stippling patterns indicate that the slope value is statistically significant in the 90% confidence interval according to the two-tailed t-test.

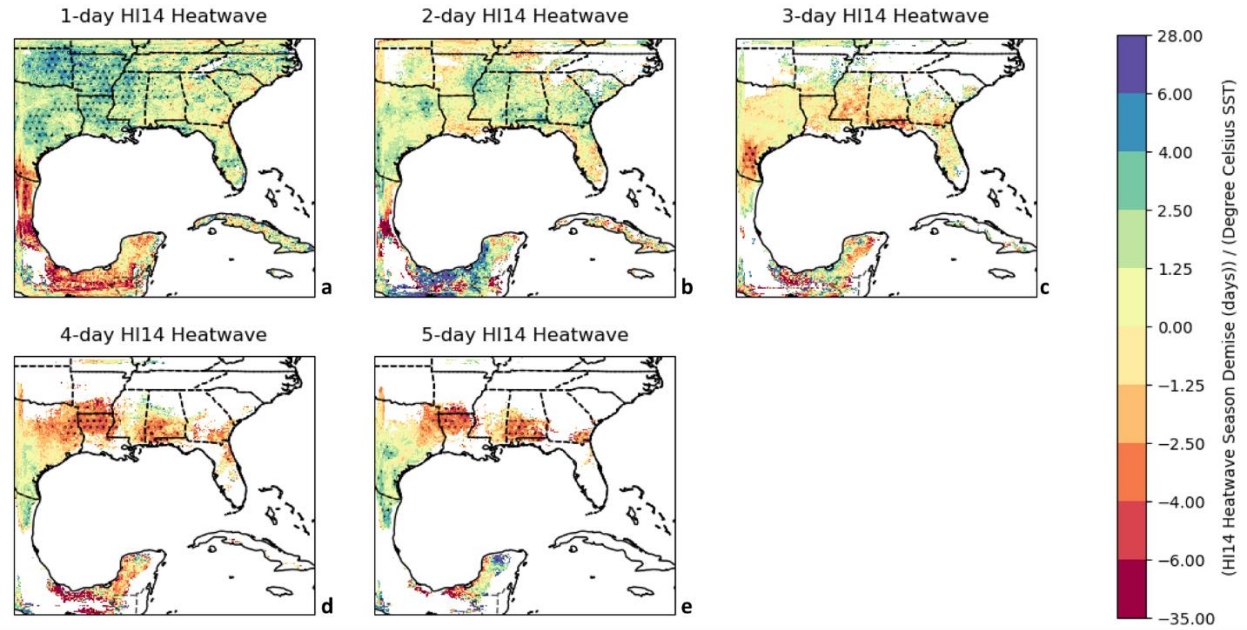

Figure 11: Linear Regression between HI14 Heatwave Season Demise (in days) and Average Degree Celsius Sea Surface Temperatures in the Nino 3.4 Region in June, July, and August over 100 years (1904 – 2004). Black stippling patterns indicate that the slope value is statistically significant in the 90% confidence interval according to the two-tailed t-test.

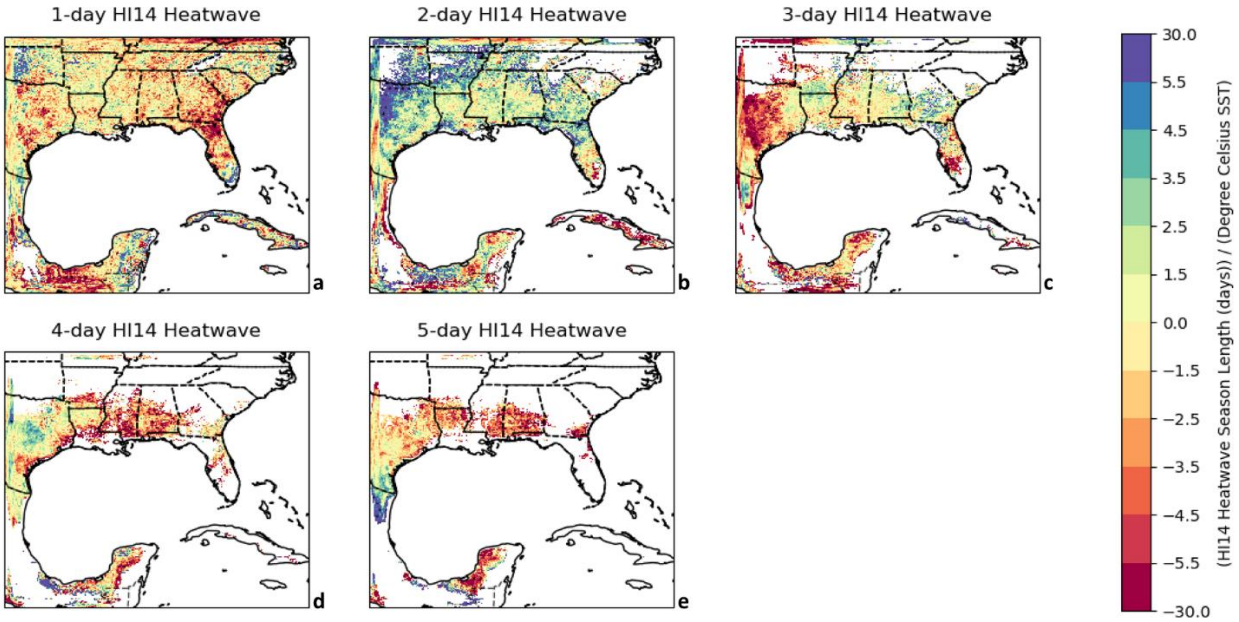

Figure 12: Linear Regression between HI14 Heatwave Season Length (in days) and Average Degree Celsius Sea Surface Temperature in the Nino 3.4 Region in June, July, and August over 100 years (1904 – 2004). Black stippling patterns indicate that the slope value is statistically significant in the 90% confidence interval according to the two-tailed t-test.

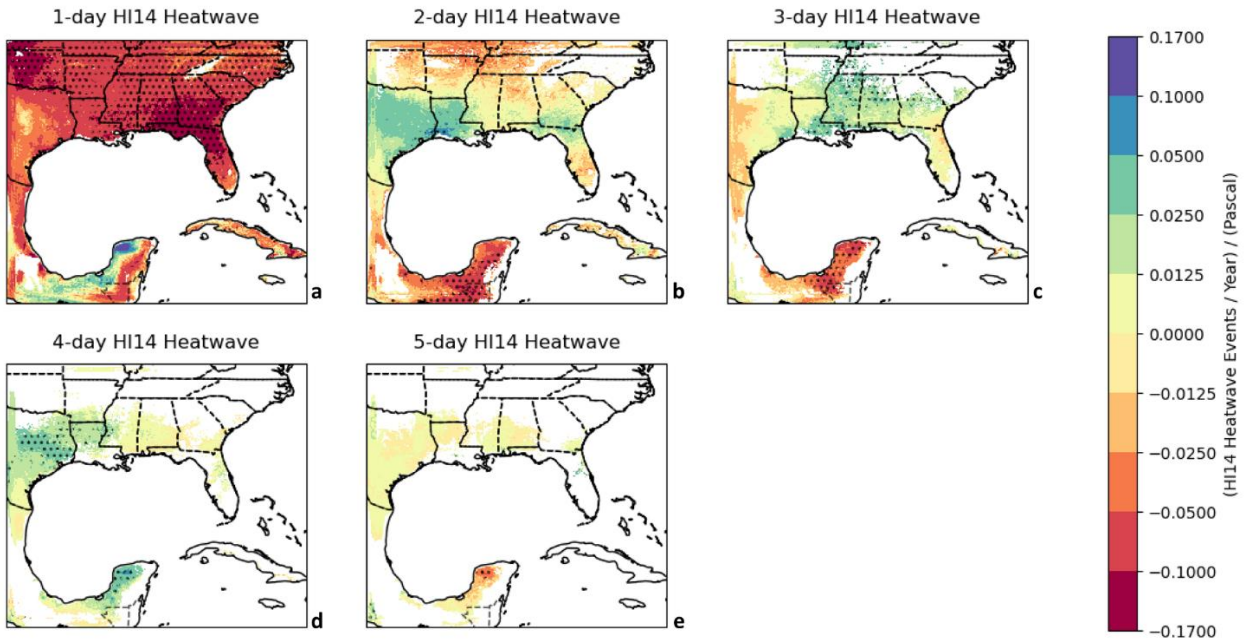

Figure 13: Linear Regression between HI14 Heatwave Events per Year and Average Sea Level Pressure (in pascals) in the Bermuda High Region in June, July, and August over 100 years (1904 – 2004). Black stippling patterns indicate that the slope value is statistically significant in the 90% confidence interval according to the two-tailed t-test.

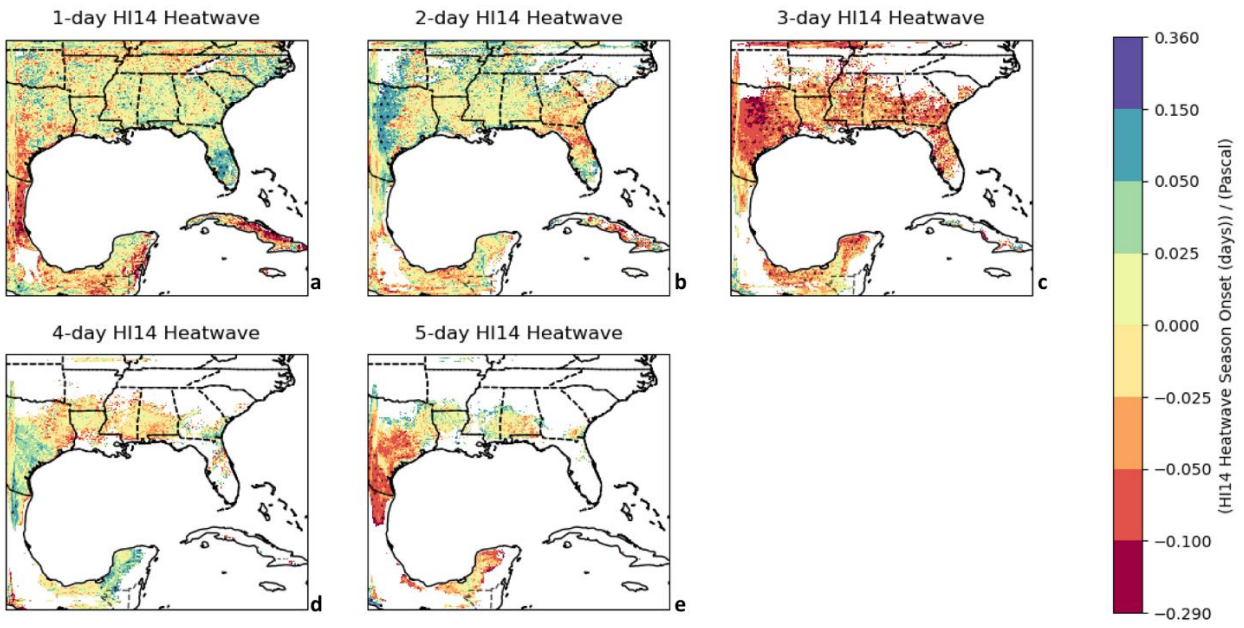

Figure 14: Linear Regression between HI14 Heatwave Season Onset (in days) and Average Sea Level Pressure (in pascals) in the Bermuda High Region in June, July, and August over 100 years (1904 – 2004). Black stippling patterns indicate that the slope value is statistically significant in the 90% confidence interval according to the two-tailed t-test.

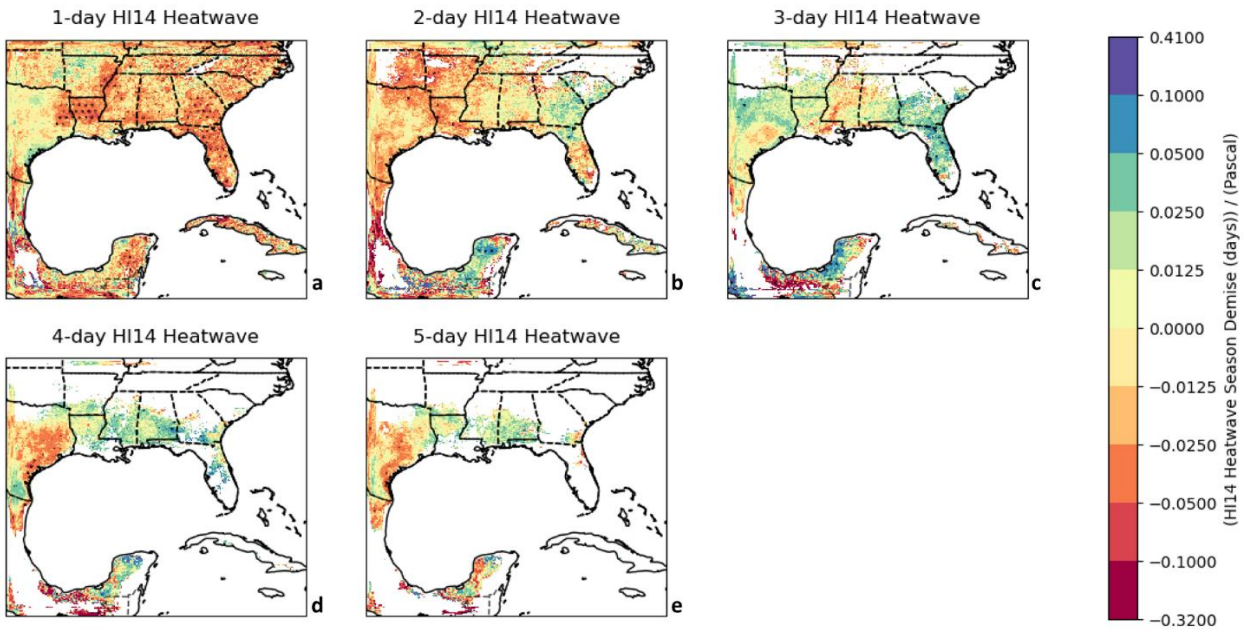

Figure 15: Linear Regression between HI14 Heatwave Season Demise (in days) and Average Sea Level Pressure (in pascals) in the Bermuda High Region in June, July, and August over 100 years (1904 – 2004). Black stippling patterns indicate that the slope value is statistically significant in the 90% confidence interval according to the two-tailed t-test.

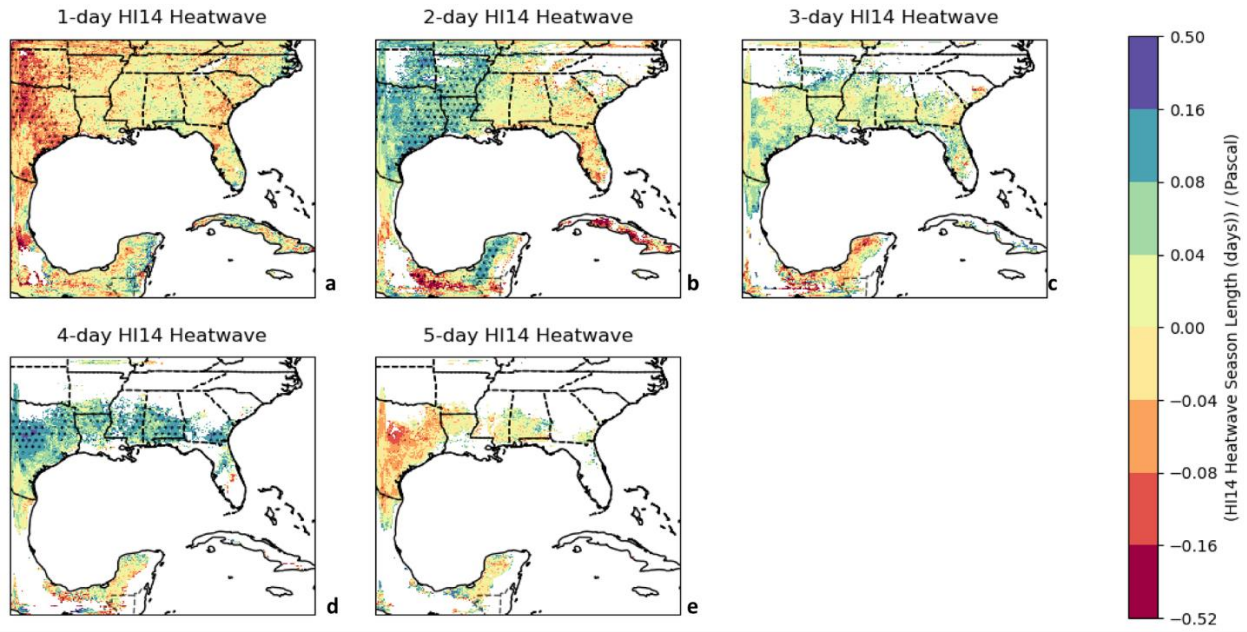

Figure 16: Linear Regression between HI14 Heatwave Season Length (in days) and Average Sea Level Pressure (in pascals) in the Bermuda High Region in June, July, and August over 100 years (1904 – 2004). Black stippling patterns indicate that the slope value is statistically significant in the 90% confidence interval according to the two-tailed t-test.

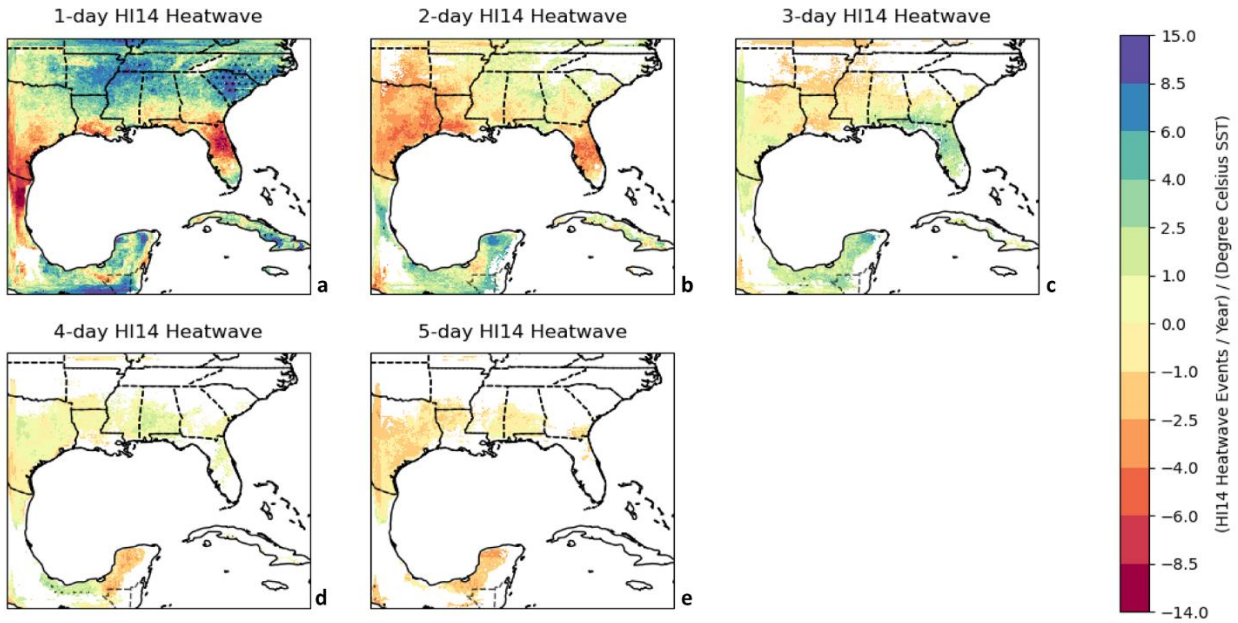

Figure 17: Linear Regression between HI14 Heatwave Events per Year and Average Degree Celsius Sea Surface Temperature Gradient between the Atlantic and East Pacific Ocean (Atlantic SST minus East Pacific SST) in March, April, and May over 100 years (1904 – 2004). Black stippling patterns indicate that the slope value is statistically significant in the 90% confidence interval according to the two-tailed t-test.

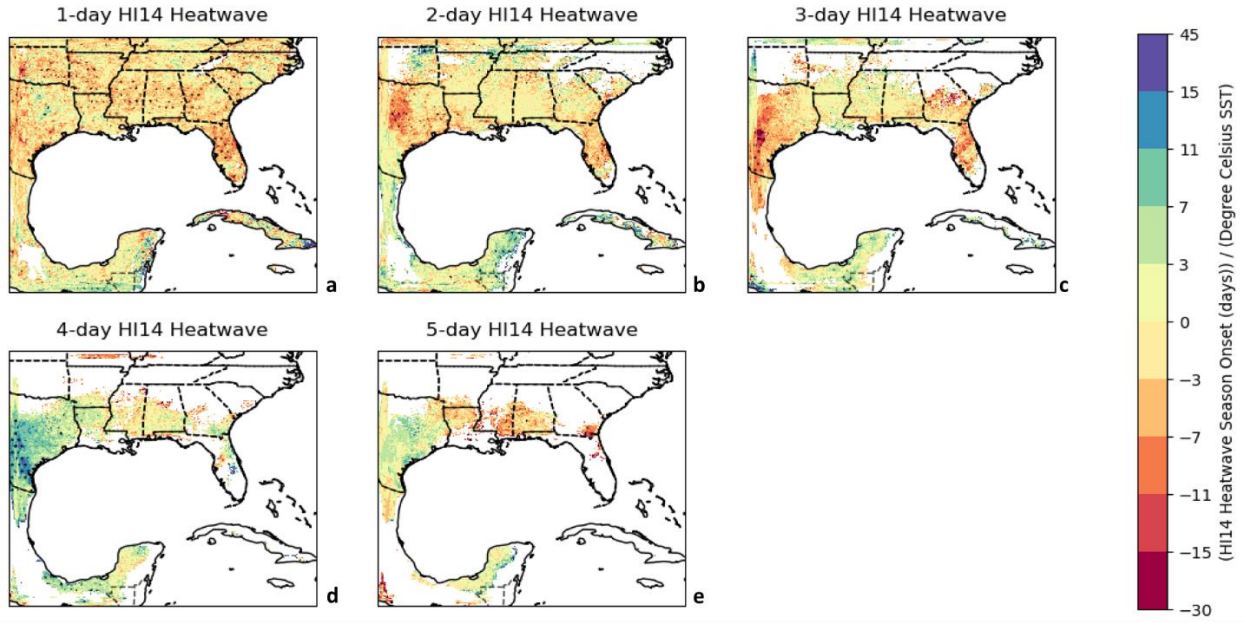

Figure 18: Linear Regression between HI14 Heatwave Season Onset (in days) and Average Degree Celsius Sea Surface Temperature Gradient between the Atlantic and East Pacific Ocean (Atlantic SST minus East Pacific SST) in March, April, and May over 100 years (1904 – 2004). Black stippling patterns indicate that the slope value is statistically significant in the 90% confidence interval according to the two-tailed t-test.

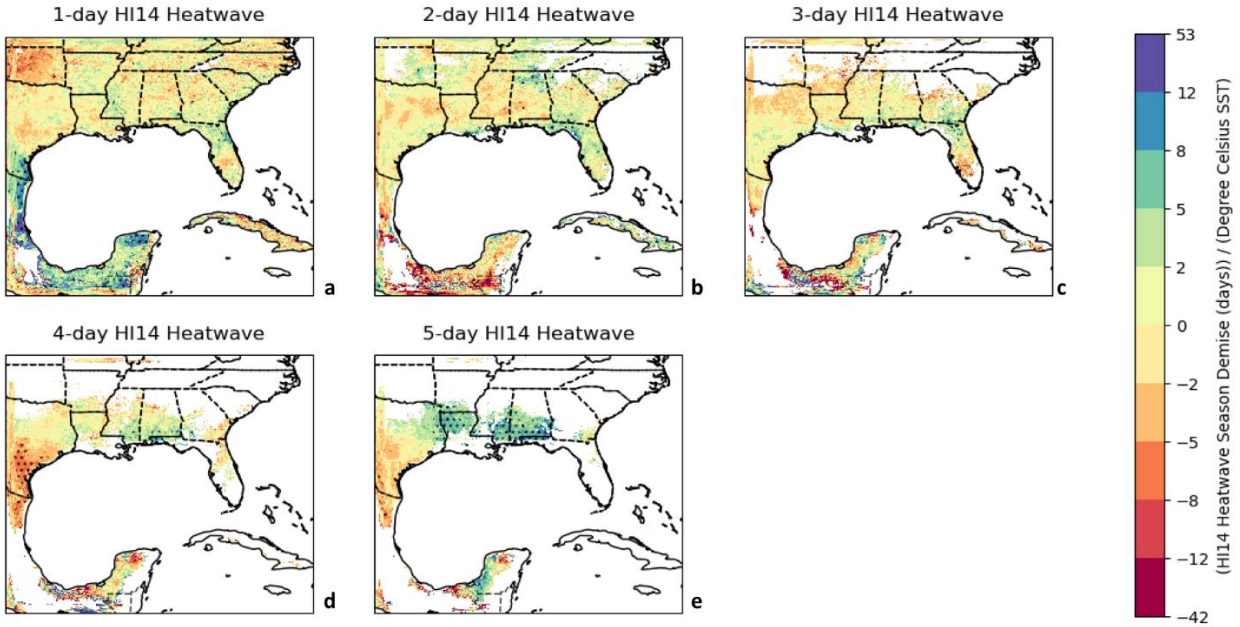

Figure 19: Linear Regression between HI14 Heatwave Season Demise (in days) and Average Degree Celsius Sea Surface Temperature Gradient between the Atlantic and East Pacific Ocean (Atlantic SST minus East Pacific SST) in March, April, and May over 100 years (1904 – 2004). Black stippling patterns indicate that the slope value is statistically significant in the 90% confidence interval according to the two-tailed t-test.

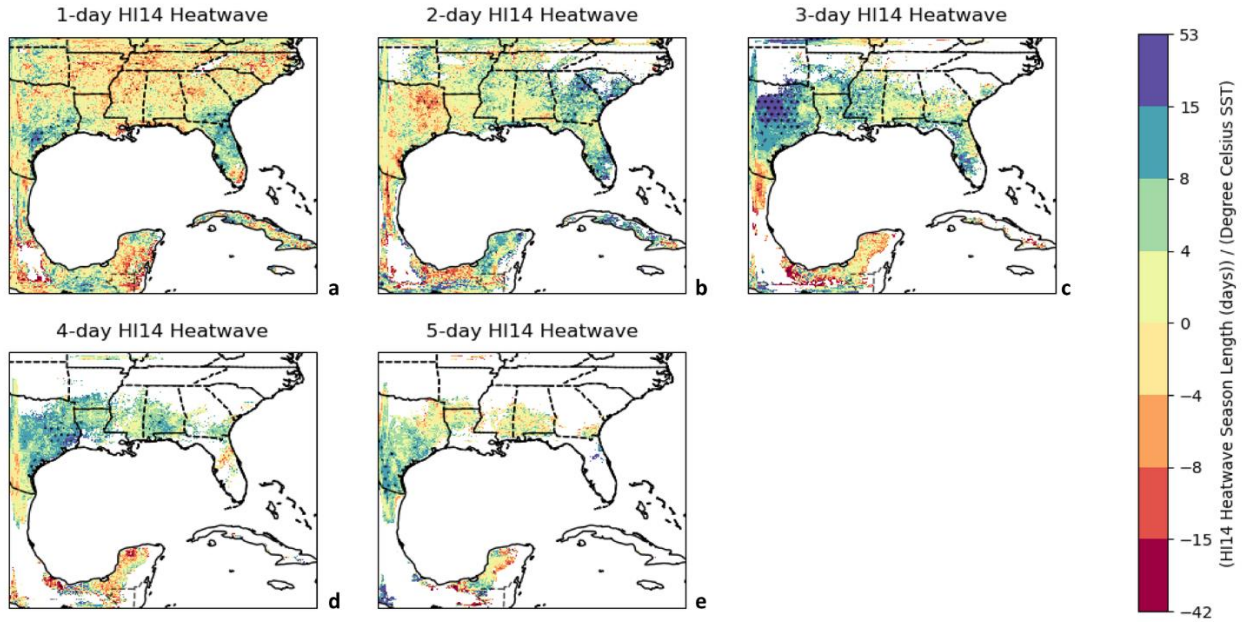

Figure 20: Linear Regression between HI14 Heatwave Season Length (in days) and Average Degree Celsius Sea Surface Temperature Gradient between the Atlantic and East Pacific Ocean (Atlantic SST minus East Pacific SST) in March, April, and May over 100 years (1904 – 2004). Black stippling patterns indicate that the slope value is statistically significant in the 90% confidence interval according to the two-tailed t-test.

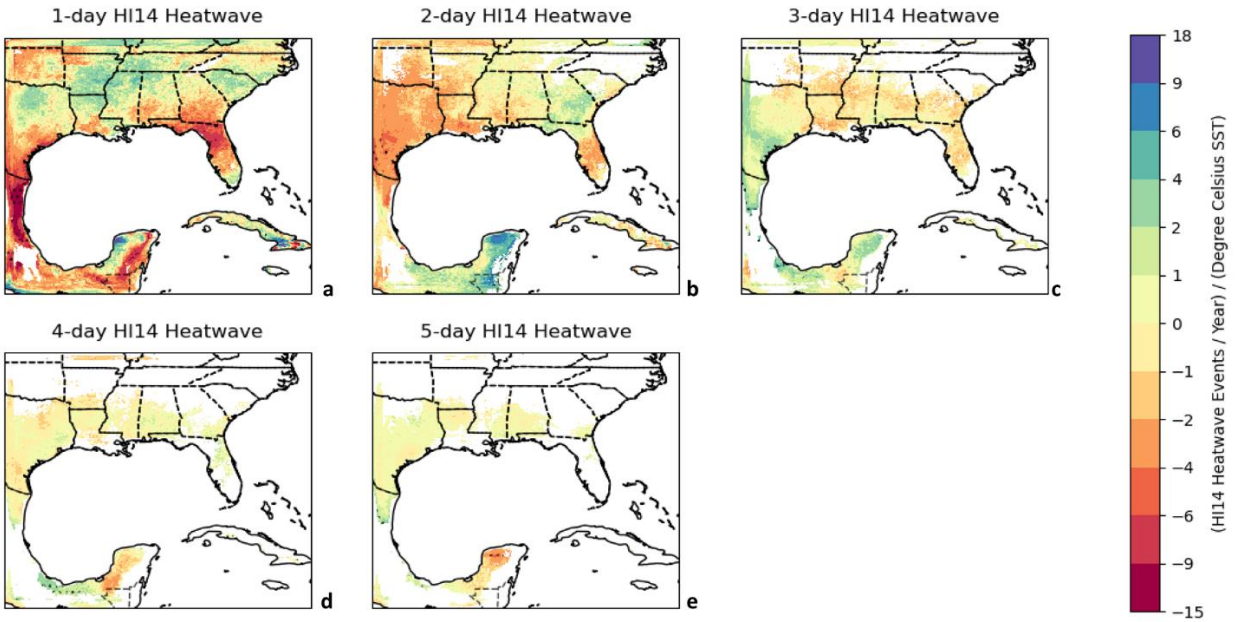

Figure 21: Linear Regression between HI14 Heatwave Events per Year and Average Degree Celsius Sea Surface Temperature Gradient between the Atlantic and East Pacific Ocean (Atlantic SST minus East Pacific SST) in June, July, and August over 100 years (1904 – 2004). Black stippling patterns indicate that the slope value is statistically significant in the 90% confidence interval according to the two-tailed t-test.

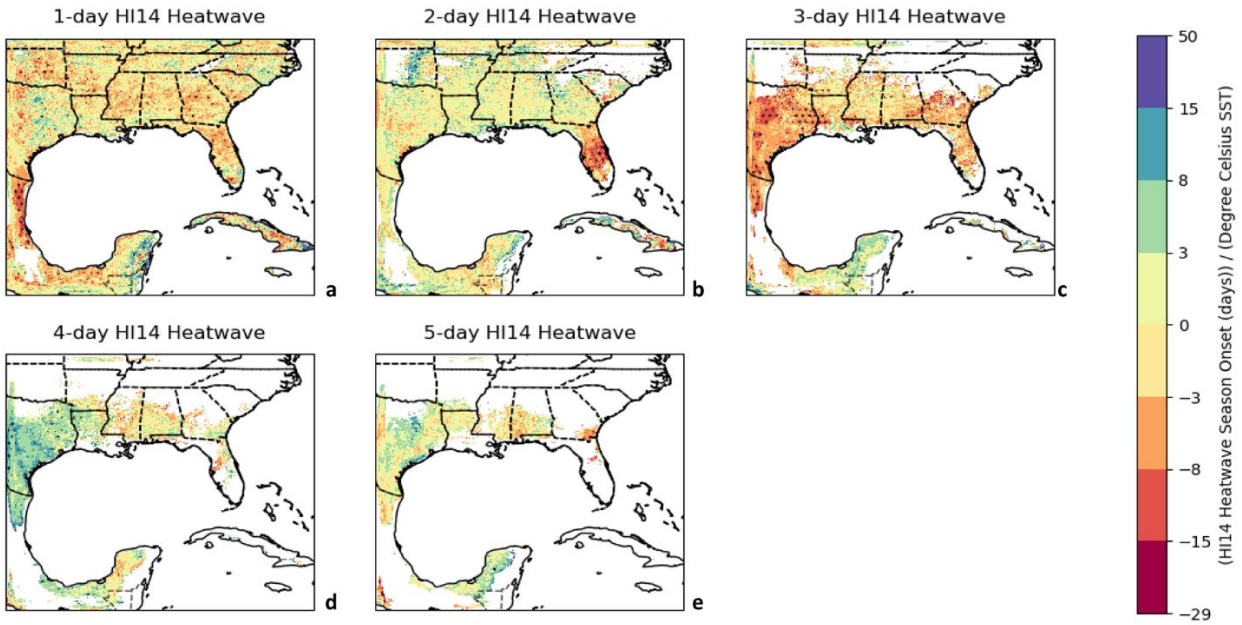

Figure 22: Linear Regression between HI14 Heatwave Season Onset (in days) and Average Degree Celsius Sea Surface Temperature Gradient between the Atlantic and East Pacific Ocean (Atlantic SST minus East Pacific SST) in June, July, and August over 100 years (1904 – 2004). Black stippling patterns indicate that the slope value is statistically significant in the 90% confidence interval according to the two-tailed t-test.

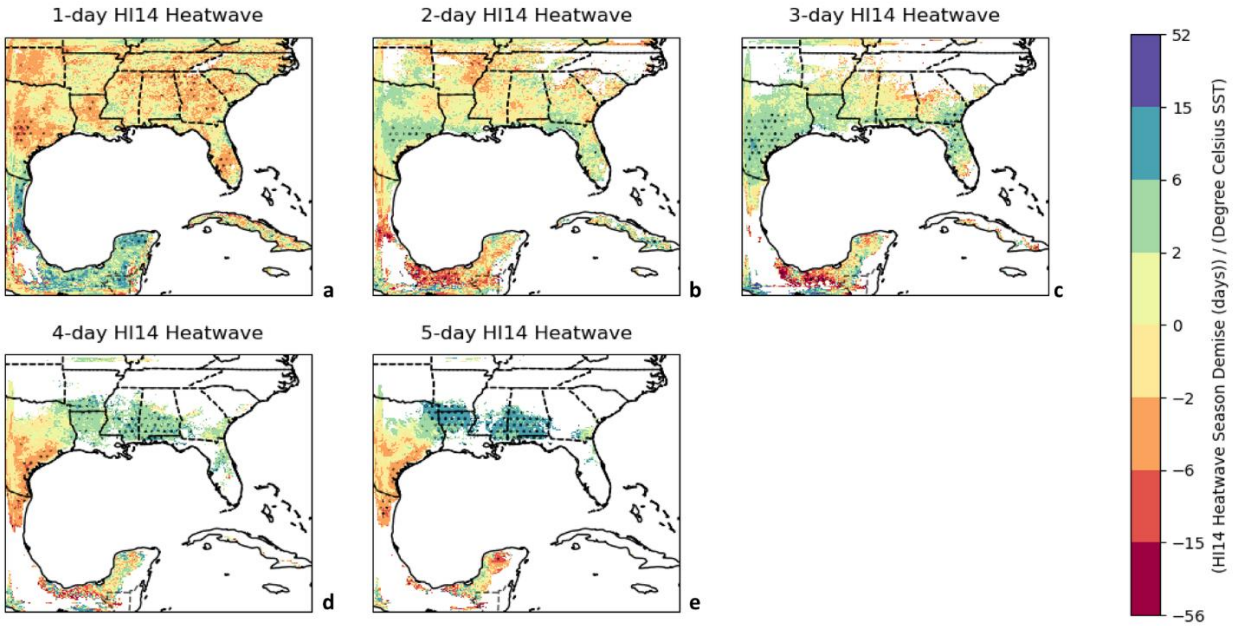

Figure 23: Linear Regression between HI14 Heatwave Season Demise (in days) and Average Degree Celsius Sea Surface Temperature Gradient between the Atlantic and East Pacific Ocean (Atlantic SST minus East Pacific SST) in June, July, and August over 100 years (1904 – 2004). Black stippling patterns indicate that the slope value is statistically significant in the 90% confidence interval according to the two-tailed t-test.

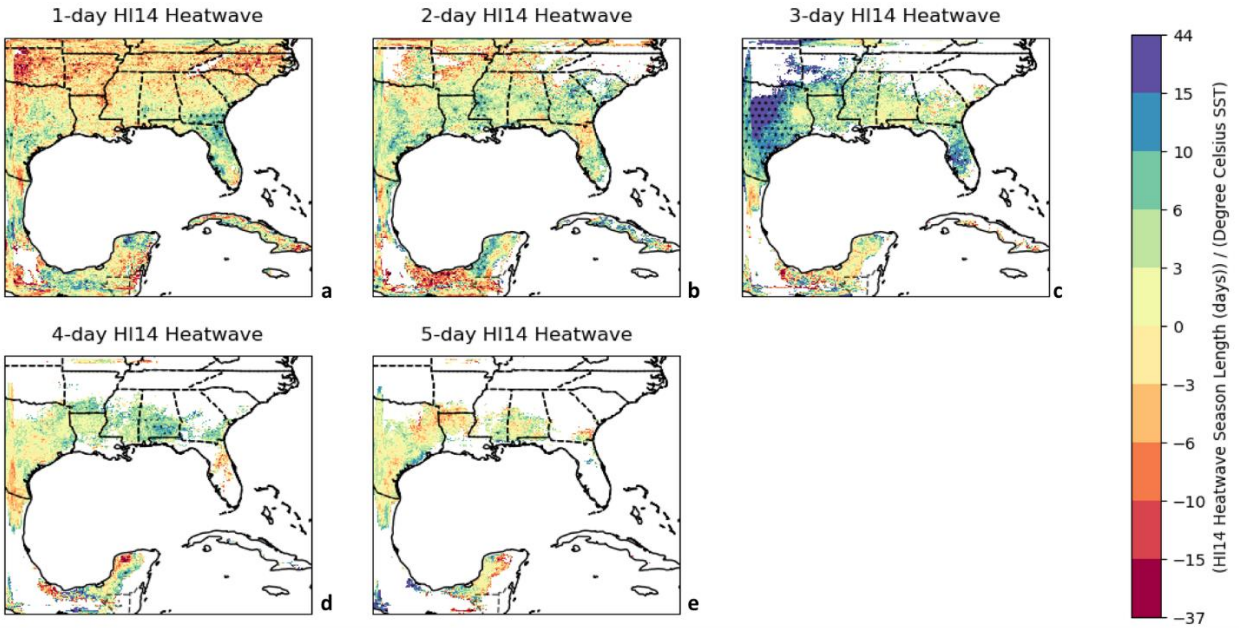

Figure 24: Linear Regression between HI14 Heatwave Season Length (in days) and Average Degree Celsius Sea Surface Temperature (SST) Gradient between the Atlantic and East Pacific Ocean (Atlantic SST minus East Pacific SST) in June, July, and August over 100 years (1904 – 2004). Black stippling patterns indicate that the slope value is statistically significant in the 90% confidence interval according to the two-tailed t-test.

8. APPENDIX

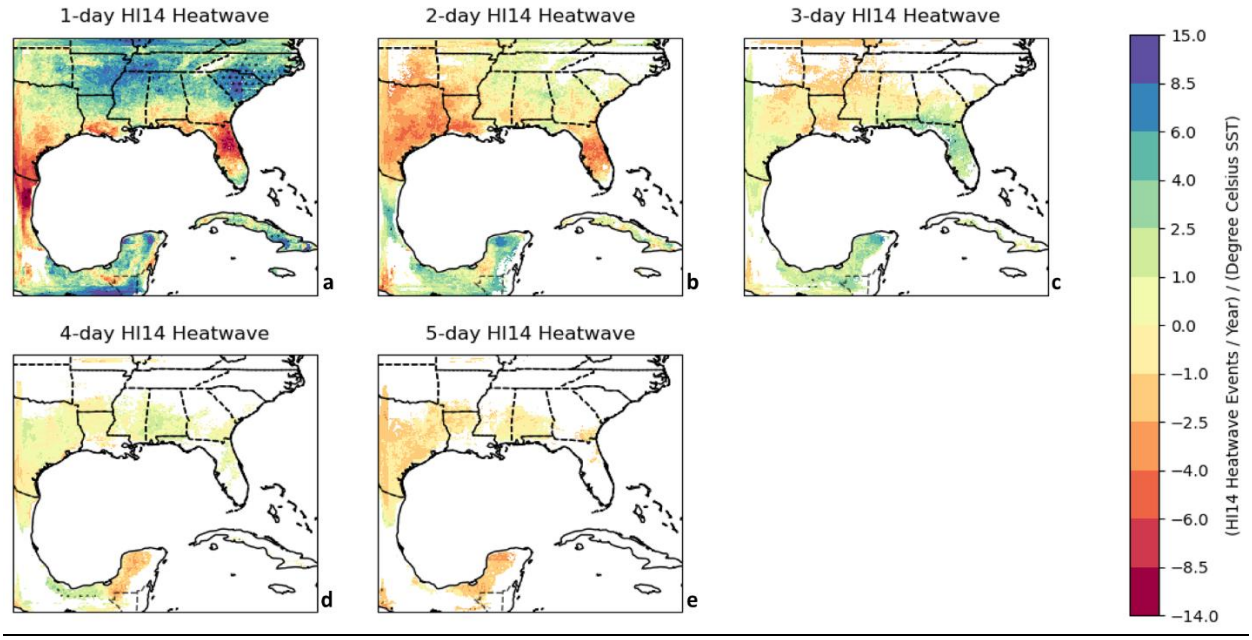

Figure 1.A: Linear Regression between HI14 Heatwave Events per Year and Average Degree Celsius Sea Surface Temperature (SST) Anomaly Gradient between the Atlantic and East Pacific Ocean (Atlantic SST anomaly minus East Pacific SST anomaly) in March, April, and May over 100 years (1904 – 2004). Black stippling patterns indicate that the slope value is statistically significant in the 90% confidence interval according to the two-tailed t-test.

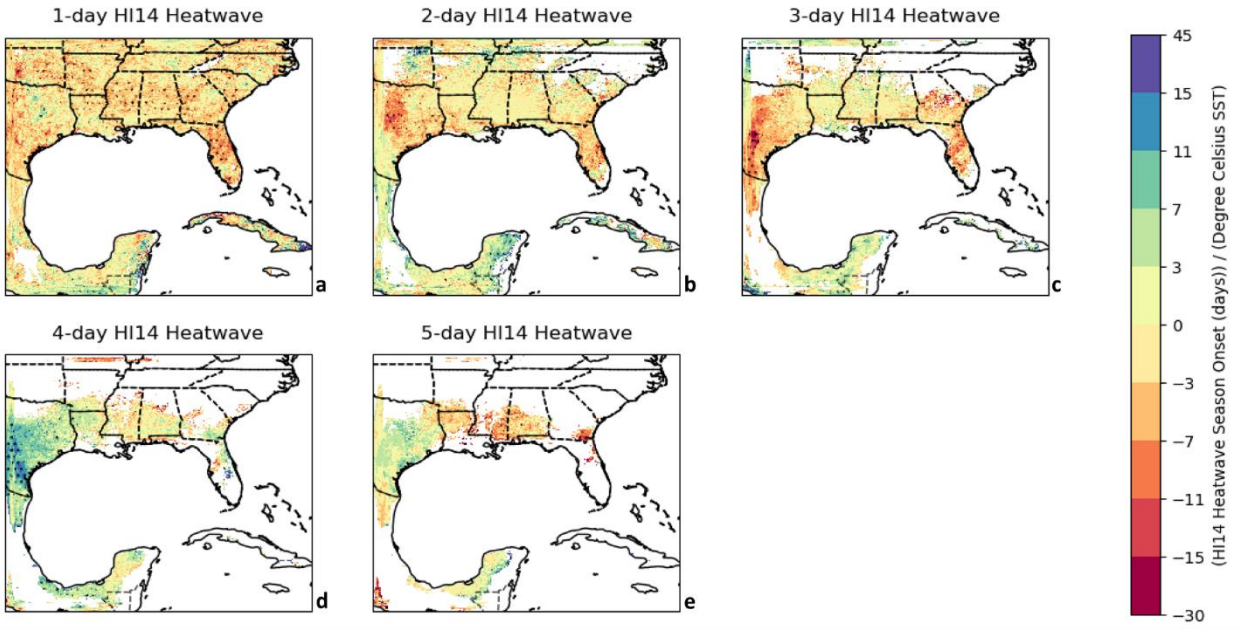

Figure 2.A: Linear Regression between HI14 Heatwave Season Onset (in days) and Average Degree Celsius Sea Surface Temperature (SST) Anomaly Gradient between the Atlantic and East Pacific Ocean (Atlantic SST anomaly minus East Pacific SST anomaly) in March, April, and May over 100 years (1904 – 2004). Black stippling patterns indicate that the slope value is statistically significant in the 90% confidence interval according to the two-tailed t-test.

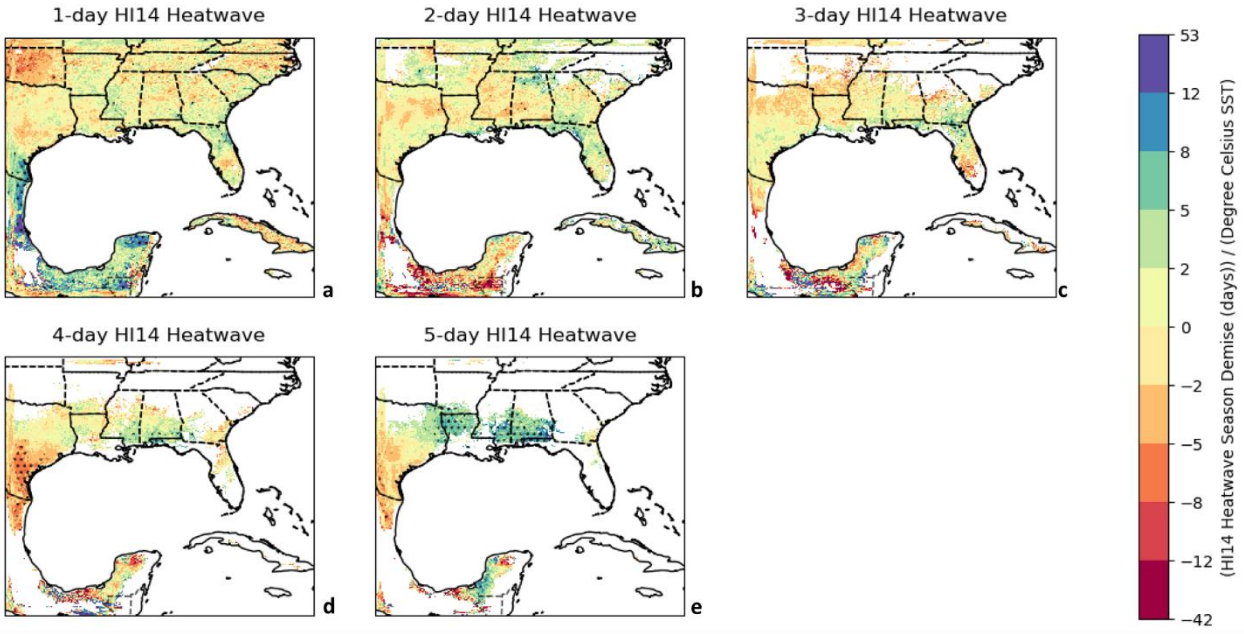

Figure 3.A: Linear Regression between HI14 Heatwave Season Demise (in days) and Average Degree Celsius Sea Surface Temperature (SST) Anomaly Gradient between the Atlantic and East Pacific Ocean (Atlantic SST anomaly minus East Pacific SST anomaly) in March, April, and May over 100 years (1904 – 2004). Black stippling patterns indicate that the slope value is statistically significant in the 90% confidence interval according to the two-tailed t-test.

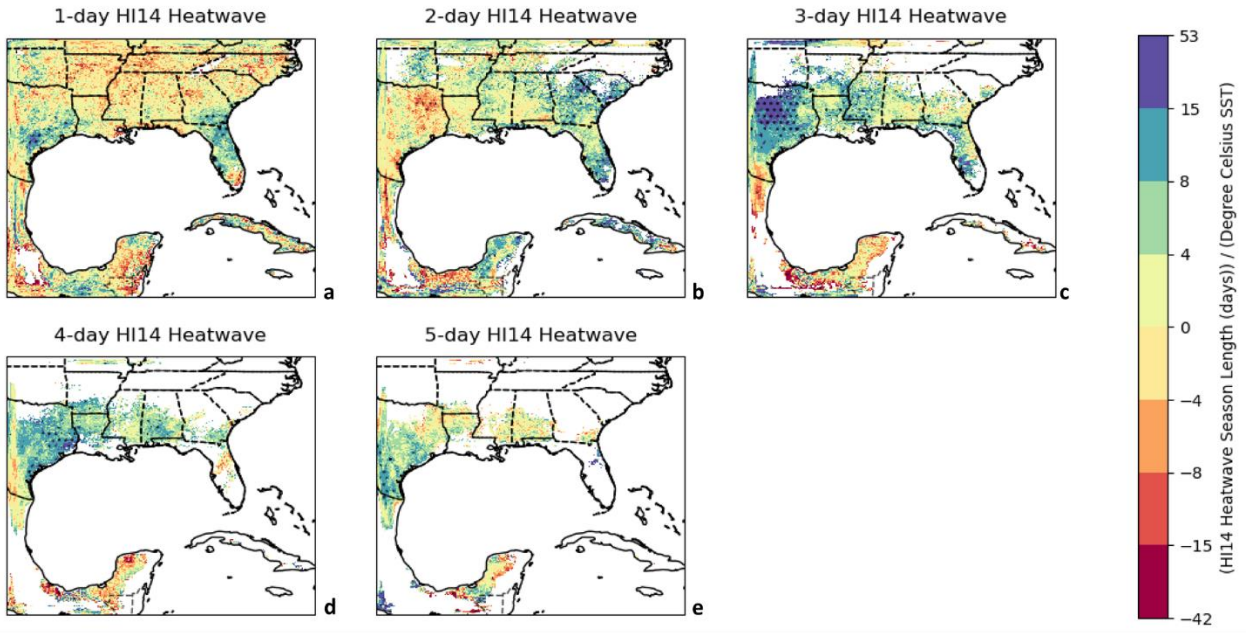

Figure 4.A: Linear Regression between HI14 Heatwave Season Length (in days) and Average Degree Celsius Sea Surface Temperature (SST) Anomaly Gradient between the Atlantic and East Pacific Ocean (Atlantic SST anomaly minus East Pacific SST anomaly) in March, April, and May over 100 years (1904 – 2004). Black stippling patterns indicate that the slope value is statistically significant in the 90% confidence interval according to the two-tailed t-test.

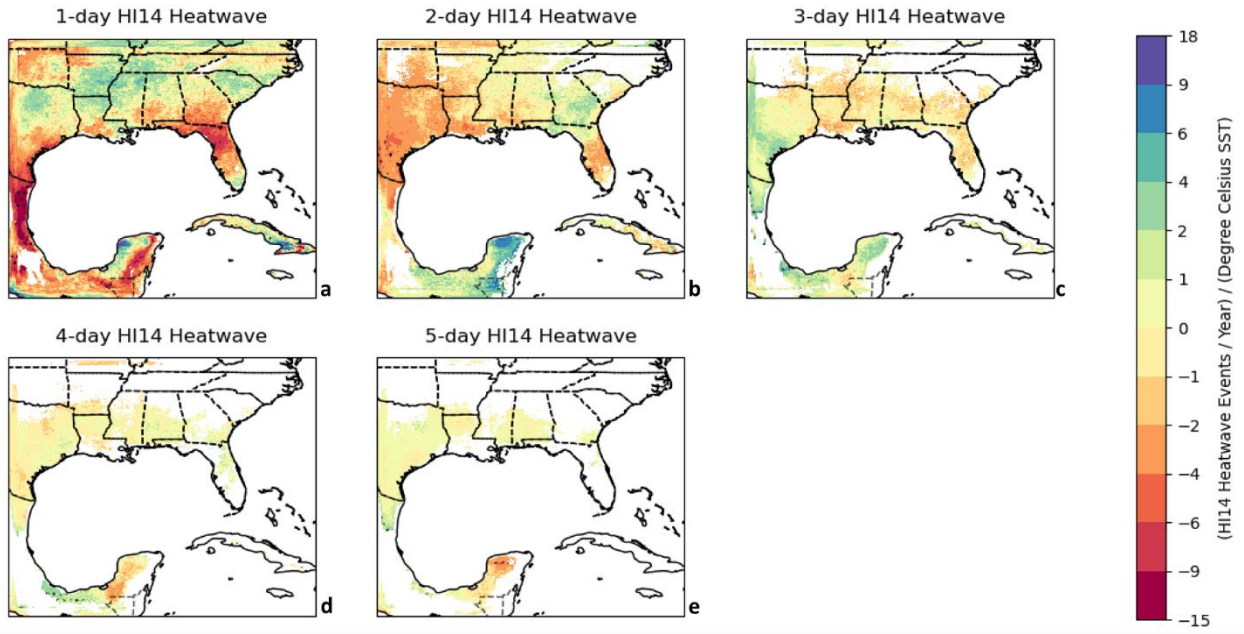

Figure 5.A: Linear Regression between HI14 Heatwave Events per Year and Average Degree Celsius Sea Surface Temperature (SST) Anomaly Gradient between the Atlantic and East Pacific Ocean (Atlantic SST anomaly minus East Pacific SST anomaly) in June, July, and August over 100 years (1904 – 2004). Black stippling patterns indicate that the slope value is statistically significant in the 90% confidence interval according to the two-tailed t-test.

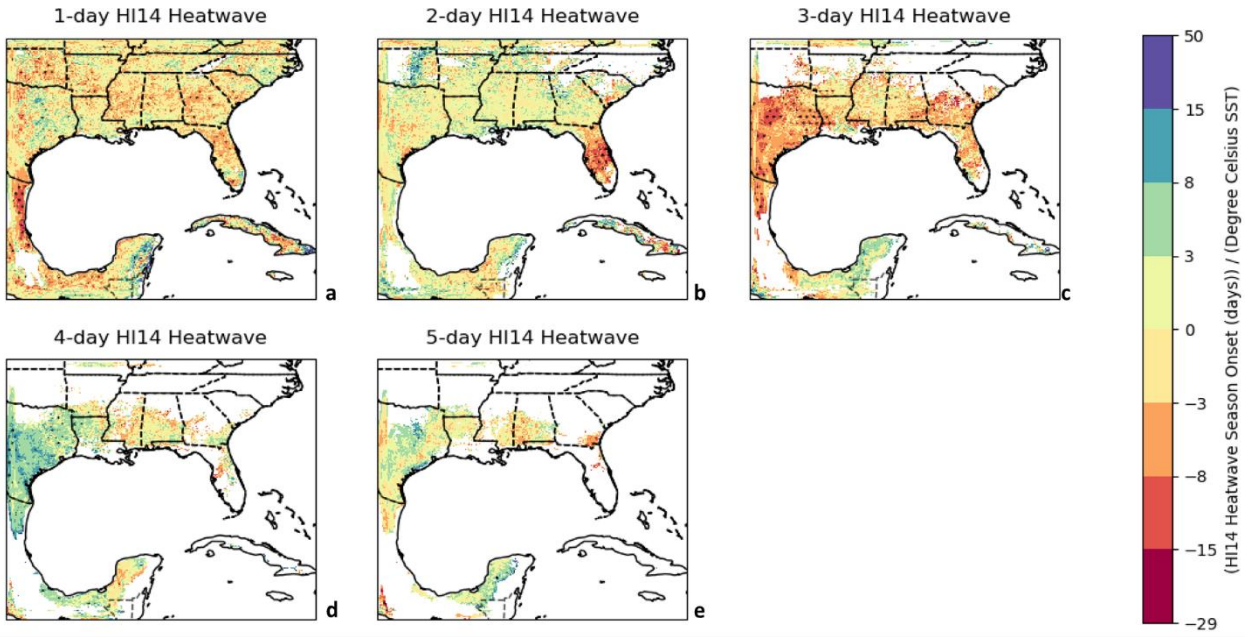

Figure 6.A: Linear Regression between HI14 Heatwave Season Onset (in days) and Average Degree Celsius Sea Surface Temperature (SST) Anomaly Gradient between the Atlantic and East Pacific Ocean (Atlantic SST anomaly minus East Pacific SST anomaly) in June, July, and August over 100 years (1904 – 2004). Black stippling patterns indicate that the slope value is statistically significant in the 90% confidence interval according to the two-tailed t-test.

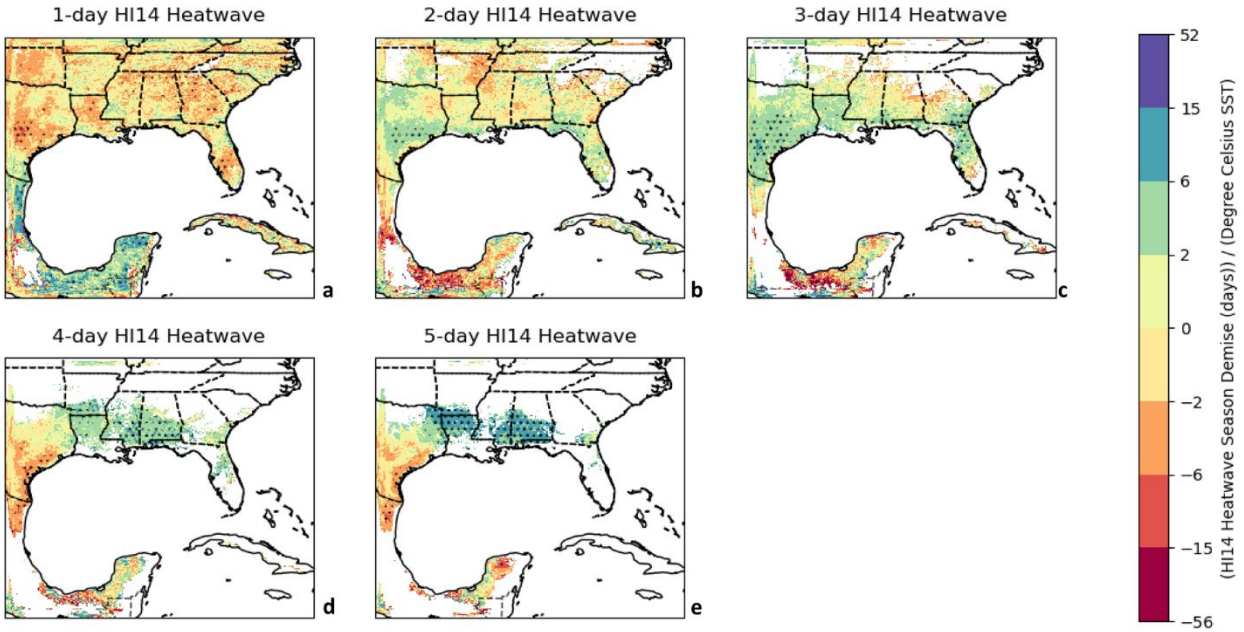

Figure 7.A: Linear Regression between HI14 Heatwave Season Demise (in days) and Average Degree Celsius Sea Surface Temperature (SST) Anomaly Gradient between the Atlantic and East Pacific Ocean (Atlantic SST anomaly minus East Pacific SST anomaly) in June, July, and August over 100 years (1904 – 2004). Black stippling patterns indicate that the slope value is statistically significant in the 90% confidence interval according to the two-tailed t-test.

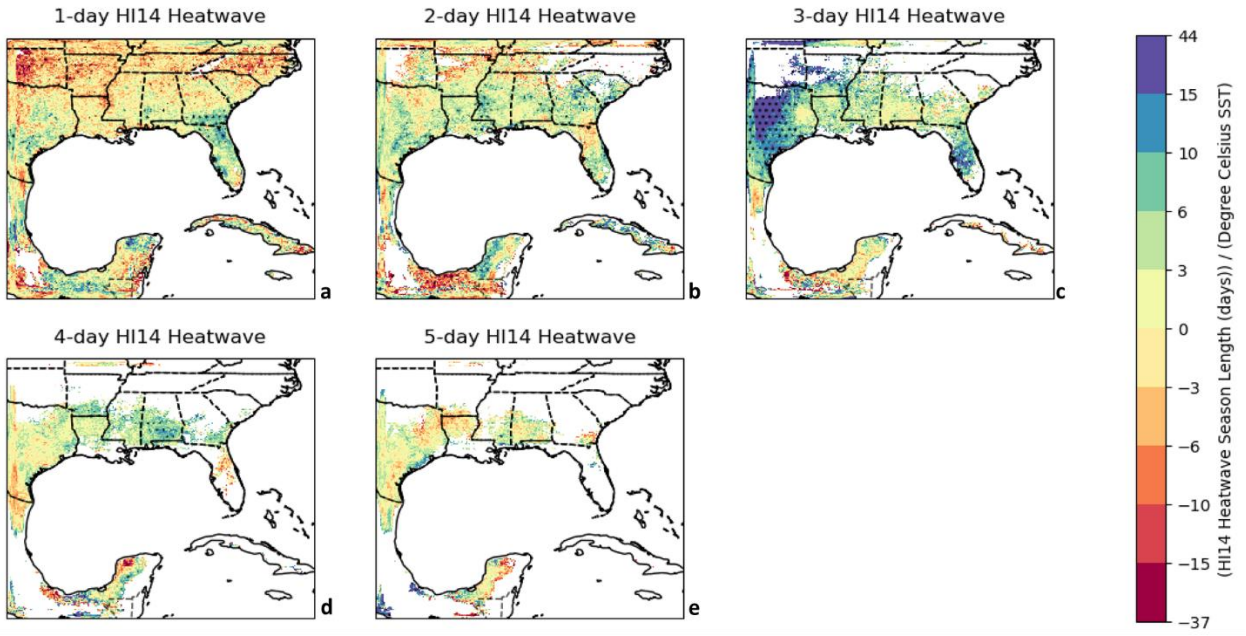

Figure 8.A: Linear Regression between HI14 Heatwave Season Length (in days) and Average Degree Celsius Sea Surface Temperature (SST) Anomaly Gradient between the Atlantic and East Pacific Ocean (Atlantic SST anomaly minus East Pacific SST anomaly) in June, July, and August over 100 years (1904 – 2004). Black stippling patterns indicate that the slope value is statistically significant in the 90% confidence interval according to the two-tailed t-test.